Storm-time Disturbed Electric Field Influence in the Strong Sporadic E-layers Occurrence over Boa Vista, a low latitude Brazilian Region

L. C. A. Resende[1,2*], S. Jiankui[1], C. M. Denardini[2], P. A. B. Nogueira[3], I. S. Batista[2], C. Arras[4], V. F. Andrioli [1,2], J. Moro[1,6], L. Silva[1,2], A. J. Carrasco[5], P. F. Barbosa[2,7], C. Wang[1], Z. Liu[1]

[1]State Key Laboratory of Space Weather, Beijing, China.

[2]National Institute for Space Research – INPE, São José dos Campos-SP, Brazil.

[3] Federal Institute of Education, Science and Technology of São Paulo, Jacarei - SP, Brazil

[4]Helmholtz Centre Potsdam, German Research Centre for Geosciences (GFZ), Department 1: Geodesy and Remote Sensing, Potsdam, Germany

[5] University of Los Andes, Mérida, Venezuela

[6]Southern Regional Space Research Center – CRS/COCRE/INPE, Santa Maria-RS, Brazil.

[7]Salesian University Center São Paulo, Campus São Joaquim, Lorena-SP, Brazil

Corresponding author: Laysa Resende (laysa.resende@inpe.br; laysa.resende@gmail.com)

Key Points:

- Anomalous Sporadic E layers that occurred in a low latitude Brazilian region, Boa Vista.
- The influence of the disturbed dynamo electric field in the strong Es layers in Boa Vista.
- The simulations allowed analyzing the electric field magnitude that caused the Es layer intensification.

Abstract

The formation of strong sporadic E-layers (Es) is frequently observed during the recovery phase of the magnetic storms over Boa Vista (BV, 2.8°N, 60.7°W), a low latitude region over the Brazilian sector. To provide some explanation for this behavior, we investigated in details the ionospheric response to the disturbed electric fields in these atypical Es layers appearance during the magnetic storm of 21-22 January 2016. The analysis was based on F region and Es layers ionospheric parameters obtained from digisonde, as well as on the Total Electron Content (TEC) obtained from Global Navigation Satellite System (GNSS). Furthermore, a theoretical model for the E region named MIRE is used to simulate the Es layers development. Such simulation takes into account the E region winds and electric fields. The results show that the storm time electric field is enough to drive the strong Es layers development. Moreover, it is seen that the intensification of the Es layers is related to the inhibition of the F-region pre-reversal enhancement of the vertical drift due to a westward electric field during the disturbance dynamo effect. Finally, the combined results from the model and observational data seemed to contribute significantly to advance our understanding of the role of the electric fields in the Es layer formation.

1 Introduction

Sporadic E (Es) layers are denser and thin layers which are mainly formed by the wind-shear mechanism in low/mid-latitudes [*Whitehead, 1961; Mathews, 1998; Haldoupis, 2011*]. The metallic ions of meteoric origin are accumulated at the null points of the winds causing density enhancement at E-region heights. Although these layers are named sporadic, they could be considered as permanent layers due to its frequent observation and the long lifetime of the metallic ions, such as Fe^+, Mg^+, K^+, Ca^+ and Na^+ [*Kopp, 1997*]. The Es layer characteristics were addressed by several authors showing that their intensity and locations are controlled generally by the tidal wind atmospheric dynamics [*Prassad et al., 2012; Pignalberi et al., 2014; Resende et al. 2017a*], and in some cases by the electric field [*Abdu et al., 2014, Resende et al. 2017b, Moro et al., 2017*].

Close to the geomagnetic equator the influence of the electric fields in the Es layer formation becomes more important since the wind shear is not the favorable mechanism in these regions. *Dagar et al. [1977]* showed that a zonal electric field component smaller than 2 mV/m could influence the Es layers formation in regions around the magnetic equator. In addition, it is well established that at equatorial regions the Es trace commonly observed on daytime ionograms is due to irregularities in the E-layers, and not a reflection from a denser layer. In fact, the diffuse and non-blanketing layer, which is classified as q-type Es or Es_q, is the manifestation of the gradient drift instability in ionograms (Type II irregularities) due to the Equatorial Electrojet Current (EEJ) [*Abdu et al., 1996; Resende et al., 2016*].

Abdu et al. [2009b] investigated the relationship between the Es layers occurrence/disruption at a low latitude location (Fortaleza) and the evening pre-reversal enhancement (PRE) in the vertical drift (or electric field) at the dip equator. They found that depending on the PRE amplitude a disruption or intensification of the Es layers could occur. *Carrasco et al. [2007]* developed a numerical model for the E region and was able to simulate that an upward (positive) vertical electric field is capable of disrupting an ongoing sporadic

layer, whereas a downward (negative) electric field favors its intensification or even formation. *Resende et al. [2016]* used the same model to analyze the electric field effect in Es layer during quiet time. They found that the electric field vertical component of the EEJ interrupts the dense layer occurrence. Also, the results confirmed that the winds are the main factor to form Es layer at low latitudes. *Moro et al. [2017]* used this same model to analyze the electric field influence in the equatorial Es layer formation during the magnetic storm that occurred in November 2004. They verified that the vertical electric fields of the EEJ irregularity suffer intense changes, disrupting the Es_q layers. Notice, however, that the electric field effect in the Es layer development at low latitudes is still poorly understood. In fact, to the best of our knowledge, there are no studies of the electric field effect in the Es layers using simulations in these latitudes.

The ionospheric zonal electric field suffers significant modifications in equatorial and low-latitude regions under disturbed conditions. These modifications/disturbances can be classified in two distinct categories: the prompt penetration electric fields (PPEFs), and the disturbance dynamo electric fields (DDEFs) [*Balan et al., 2008; Blanc and Richmond, 1980*]. The interplanetary electric field is related to the IMF B_z component of the interplanetary magnetic field and to the solar wind velocity (V_{SW}). During a southward incursion of IMF Bz, we have an undershielding electric field which penetrates into the ionosphere with eastward (westward) polarity in the day (night) side of the Earth. A reversal of the IMF Bz to north generates an overshielding condition in which the electric field is westward (eastward) during day (night), being in opposite direction do the undisturbed dynamo electric field [*Nogueira et al., 2011*]. The DDEFs, on the other hand, occur due to energy input into the high latitude ionosphere that results into Joule heating and collisional interactions that drive disturbance thermospheric winds toward the equator, creating a disturbed dynamo electric field. They generally occur a few hours after the energy input at high latitudes, generally during the later phases of the geomagnetic storms and have opposite direction to the quiet time electric fields [*Santos et al., 2016*]. In both cases, the disturbed electric fields alter the F region plasma in the ionosphere and can cause some modification in the Es layers as well [*Abdu et al., 2009b*].

This paper analyzes the strong Es layer observed in the ionograms at a low latitude region, Boa Vista (BV, 2.8°N, 60.7°W, dip = 18º) in January 2016. We evaluate the significantly enhanced Es layer during the recovery phase of a magnetic storm, in which we attributed such enhancement to the DDEF influence. We used an Es layer numerical model, named MIRE, with a novel neutral wind input to analyze the electric field influence in the Es layer formation over the BV region. Finally, we present a deep study of the possible causes of such strong Es layers that are occurring in BV using simulations and measurements obtained from the ionosondes.

2 Ionospheric Data and Modeling

Data from digisonde (DPS-4D) are collected and analyzed in order to get information on F-layer and Es parameters at BV and other stations: Campo Grande (CG, 20.5°S, 55°W, dip = -17º), São Luís (SLZ, 2.5°S, 44.3°W, dip = -3.8º), and Fortaleza (FLZ, 4°S, 38°W, dip = -9º). We have also analyzed the Total Electron Content (TEC) data obtained from a network of Global Navigation Satellite System (GNSS) receivers in South America to verify the response of equatorial and low latitude ionosphere during a magnetic storm. Additionally, the Global Scale Wave Model (GSWM-00) is used as input to MIRE for the selected Brazilian regions. The

interaction of the electric fields with the Es layer dynamics was studied for the intense geomagnetic storm of January 2016. In the following, we briefly describe each set of data and models used in this work.

2.1 Digisonde Data

Digisonde is a radar that operates at frequencies ranging from 1 to 30 MHz. It generally operates continuously, making a complete sweeping every 10/15 min [*Reinisch et al., 2009*]. The data provides the ionospheric profile in graphs of frequency versus virtual height, from which it is possible to get the ionospheric parameters for the F and E regions with Es layers. In this study we used the following parameters: the Es blanketing frequency (*fb*Es), which corresponds to the frequency up to which the Es layer blocks the transmitted electromagnetic wave; and the top frequency (*ft*Es), which is the maximum frequency that was reflected from the Es layer. Furthermore, to study the magnetic storm effect in the ionosphere as a whole, we also analyzed the F regions parameters, as the height of the F- layer peak density (*hm*F2) and the vertical drift velocity (V_z).

The V_z is obtained by the relation $\Delta hF/\Delta t$, in which the hF is calculated using true heights at specific plasma frequencies 4, 5, and 6 MHz. In fact, we used the mean of the drift values calculated at the three frequencies, which was used to represent the height averaged vertical drift of the bottom side F region. More details about this methodology can be found in *Abdu et al. [2010]*.

It is important to emphasize that all the ionospheric parameters derived from digisonde data were manually checked since significant discrepancies can be found between the automatically scaled and the true values at Brazilian region. Additionally, further information on the ionosonde model, data availability, and other parameters related to these ionospheric observatories can be found in the review by *Denardini et al. [2016]*.

2.2 GNSS TEC Variation

The frequency radio signals from the GNSS receiver measures the total number of electrons (TEC) in a column of unit cross-section area between the satellite and the receiver. The TEC values are made available at the website of the Brazilian Studies and Monitoring of Space Weather (Embrace - http://www2.inpe.br/climaespacial/portal/en/), which produces the ionospheric maps. Specifically, we have obtained two-dimensional maps of the absolute vertical TEC values at 10 min time resolution and 0.5°×0.5° of spatial resolution in latitude and longitude in this analysis. The methodology was developed by *Otsuka et al. [2002]*, and the description for the Brazilian sector can be found in *Takahashi et al. [2016]*.

2.3 MIRE Model

We simulated the Es layers using a theoretical model, called MIRE (the Portuguese acronym for E-Region Ionospheric Model), which provides the E region electron density. This is accomplished by solving a system of differential equations of the continuity and momentum for the molecular/atomic (NO^+, O_2^+, N_2^+, O^+) and metallic (Fe^+, Mg^+) ions. The system was solved

using 0.05 km grid spacing in height, and 2 min time step between 00 LT and 24 LT. In this analysis, we used the height range from 86 to 120 km. Notice that MIRE can be used for heights up to 140 km, but the GSWM-00, which is used to calculate the input winds for MIRE, does not provide data above 120 km, which is the source of the altitude limitation of this study. More details about the equations and implementation of MIRE can be seen in *Carrasco et al. [2007]* and *Resende et al. [2017a]*.

The Es layers formation dynamics can be analyzed by the vertical velocity of the ions:

$$V_{iz} = \frac{\omega_i^2}{(v_{in}^2 + \omega_i^2)}\left[cos\, I \cdot sin\, I \cdot U_X + \frac{v_{in}}{\omega_i} \cdot cos\, I \cdot U_y + \frac{1}{v_{in}}\frac{e}{m_i} \cdot cos\, I \cdot sin\, I \cdot E_x + \frac{e}{\omega_i m_i} \cdot cos\, I \cdot E_y + \frac{e}{v_{in} m_i} \cdot \left(\frac{v_{in}^2}{\omega_i^2} + sin^2 I\right) \cdot E_z\right] \quad (5)$$

where ω_i is the ion gyrofrequency, v_{in} is the ion-neutral collision frequency, I is the magnetic inclination angle, m_i is the mass of the ion, e is the electric charge of the ion, E_x, E_y, and E_z, are the electric field components, and U_x is the meridional and U_y is the zonal wind components in the E region. Here, the X-axis points towards the south, the Y-axis points towards the east, whereas the Z-axis completes the right-handed coordinate system, pointing up.

In the previous works that used MIRE, the wind model was obtained by the fitting of amplitude, wavelength, and phase parameters computed from the observational data of the meteor radar installed in Brazilian low-latitude regions [*Resende et al., 2016; Resende et al., 2017a; Resende et al., 2017b; Moro et al., 2017*]. However, there is no meteor radar available near BV. Thus, in the present study, it was necessary to use a theoretical model, the GSWM-00, which successfully described the wind dynamics over the regions near geographic equator [*Hagan et al., 2002, 2003, Buriti et al., 2008*]. Details about the GSWM-00 can be seen on the website of the High Altitude Observatory (HAO) of the National Center for Atmospheric Research (NCAR), in Colorado (http://web.hao.ucar.edu/public/research/tiso/gswm/gswm.html).

Using GSWM-00, we obtain the semidiurnal (12h) and diurnal (24h) amplitudes, the phase, and the wavelength for zonal and meridional tidal wind components in BV. Then, the tidal components can be computed by:

$$\boldsymbol{U_x(z) = U_{x0}(z) \cdot cos\left(\frac{2\pi}{\lambda_x}(z - z_0) + \frac{2\pi}{T}(t - t_{x0}(z))\right)} \quad (5)$$

$$\boldsymbol{U_y(z) = -U_{y0}(z) \cdot sin\left(\frac{2\pi}{\lambda_y}(z - z_0) + \frac{2\pi}{T}\left(t - t_{y0}(z)\right)\right)}, \quad (6)$$

where $U_{x0}(z)$ e $U_{y0}(z)$ correspond to wind amplitudes at the height z; λ_x and λ_y denote the wavelengths; T is the period of the tide (24h for diurnal and 12h for semidiurnal); z_0 is a reference height assumed as 100 km; and $t_{x0}(z)$ and $t_{y0}(z)$ are the wave phases.

Figure 1 shows the temporal and altitudinal variation of the meridional (Figure 1a) and zonal (Figure 1b) wind profiles of the tidal modes that were included in MIRE to simulate the Es layers over BV. It is important to mention here that the GSWM-00 was used as input in MIRE model for the first time, which required validation before carrying out the analysis of the electric field effects.

The null points (zero curves) indicate the wind shear mechanism that is necessary to form the Es layer. The zonal amplitude is larger (max ~ 25 m/s) than the meridional amplitude (max ~ 17 m/s), in agreement with the observational results obtained previously for other Brazilian regions [*Resende et al., 2017a; Resende et al., 2017b*]. However, the wind amplitudes are lower in BV than at other Brazilian regions analyzed before. Hence, it is expected the Es layers to be very weak in BV in most days, which agrees with the numerical results obtained from MIRE as will be shown in Section 3.

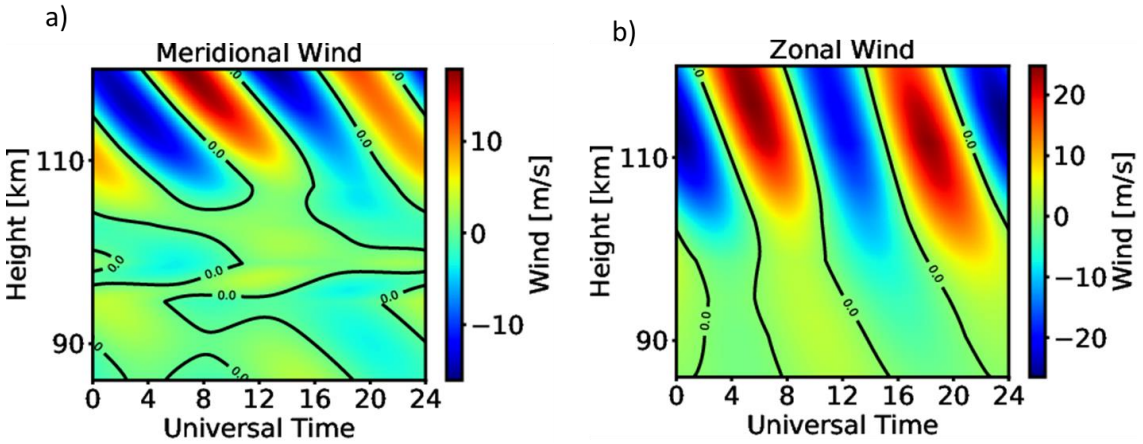

Figure 1. Wind profile of the meridional (a) and zonal (b) obtained by GSWM that was included in MIRE to simulate the Es layers over BV.

3 Results and Discussion

3.1 Magnetic storm Event

Figure 2 shows the variations of the interplanetary magnetic field (IMF) B_z component (a), the solar wind speed (V_{SW}, km/s) (b), the Dst index (nT) (c), and AE, auroral electrojet (nT) index (d) for the 18-25 January 2016 geomagnetic storm. The B_z and V_{SW} parameters were taken from the OMNIWeb database, which were obtained from the Advanced Composition Explorer

(ACE) satellite measurements. The AE and Dst indices were obtained from the World Data Center from Geomagnetism, Kyoto.

The coronal mass ejection (CME) arrived in the Earth's magnetosphere on 19 January 2016 at 1000 UT, causing an abrupt increase in the B_z component. The CME effect lasted until January 21, 2016, when the Earth's environment starts to recover. Additionally, the Bz component turned southward (negative) from about 0530 UT on 20 January to 0400 UT on 21 January. The Dst index started to decrease (magnetic storm main phase) at around 0100 UT on 20 January, reaching almost -100 nT at 1600 UT, which is the threshold for classifying it as an intense storm according to the classification by *Gonzalez et al. [1994]*. Afterward, it is possible to observe a slow recovery of the Dst index that lasted until 23 January. The V_{SW} increased gradually from about 320 km/s to almost 600 km/s. Furthermore, the AE index showed a peak of ~1250 nT around 1500 UT on 20 January. After this peak, the AE had an oscillating behavior with values between 200 nT and 500 nT.

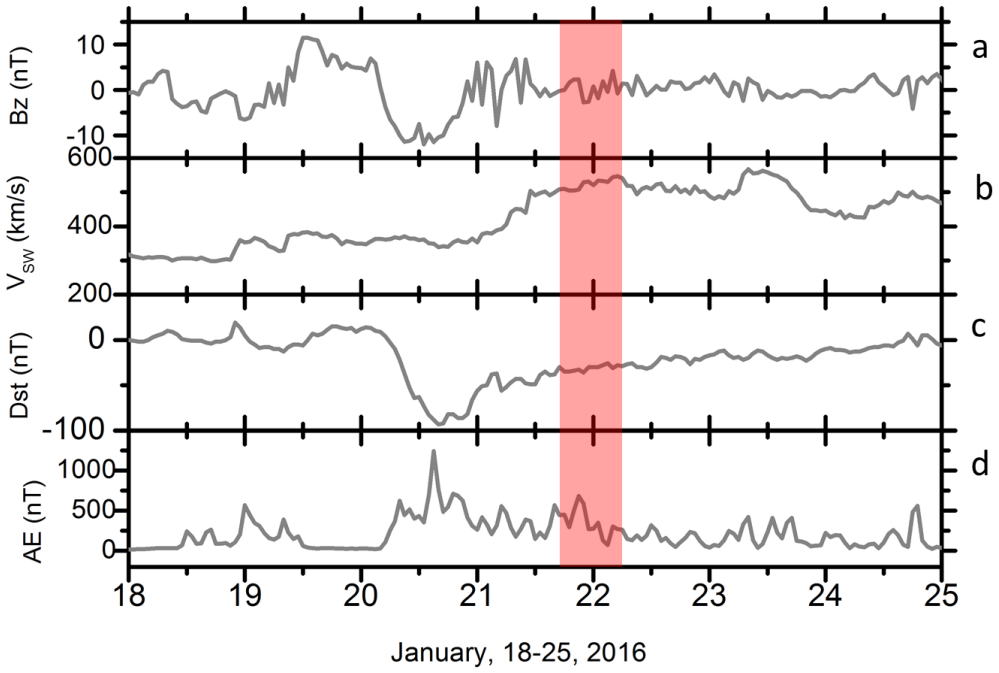

Figure 2. IMF Bz, solar wind speed, Dst, and AE auroral electrojet indices (UT) from 18 to 25 November 2016.

3.2 Strong Es layer in BV

During part of the magnetic storm recovery phase that occurred on 21-22 January 2016, we observed strong Es layers in BV, which is not the typical behavior at that location. This layer occurrence starts at 2330 UT on 21 January and it lasts until 0640 UT on 22 January, when it starts to weaken. Therefore, although we are showing the data obtained from the days around the magnetic storm that occurred on 20 January, we will focus only on the shaded area of Figure 2.

Figure 3 shows the Es layers in ionograms (red arrow) between 2330 UT on 21th and 0700 UT on 22th January 2016, in increments of half an hour. During this time, the *ft*Es oscillated between high and low values. In fact, between 2330 UT and 0100 UT, the *ft*Es reached values even higher than 15 MHz (at 0050 UT, not shown here). After, the Es layer started to weaken, but it strengthened again in the next hours (see 0300 UT). This oscillation lasted until 0700 UT, when the Es layer began to disappear. In the hours following 0700 UT, the Es layers returned to its typical behavior with a not significant density (not shown here).

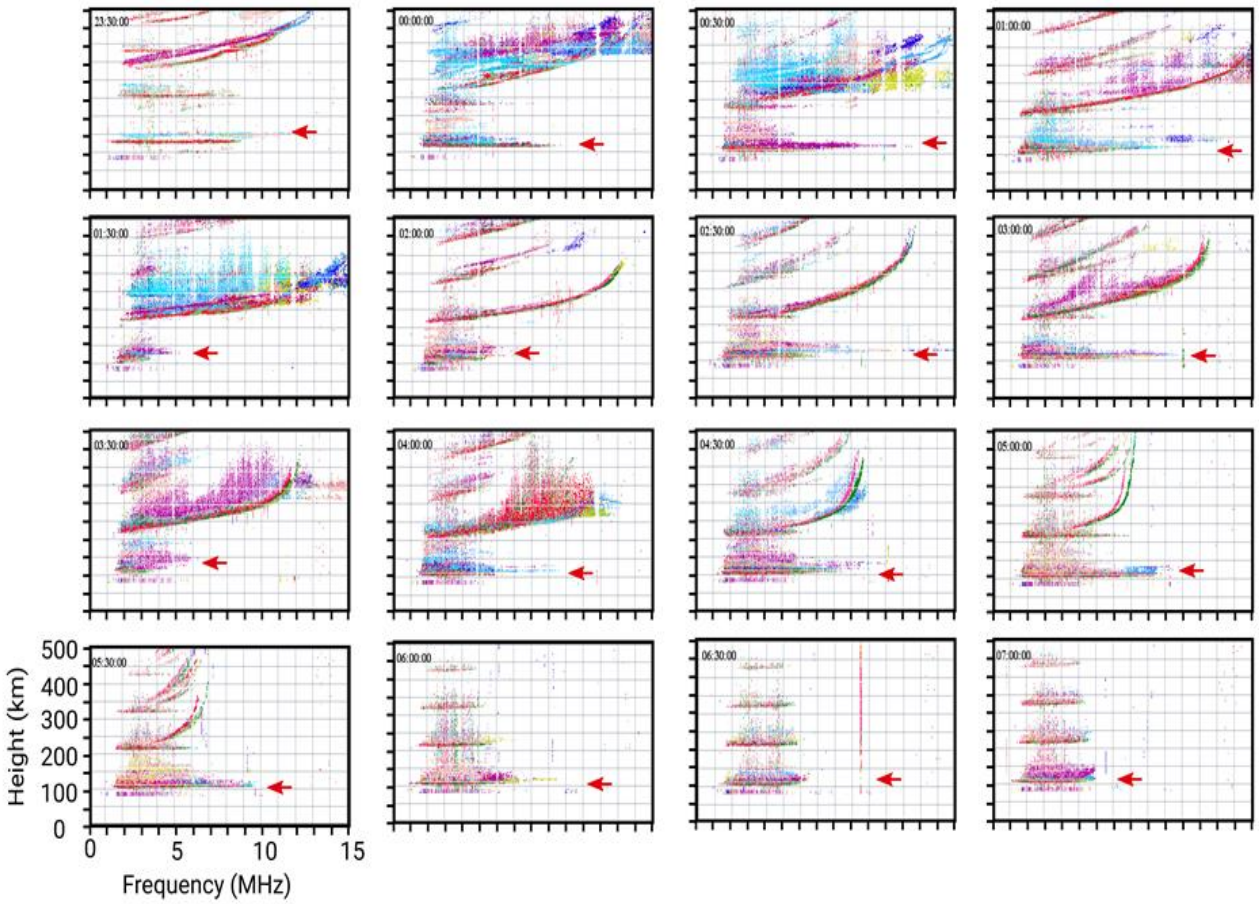

Figure 3. Ionograms at Boa Vista collected from 2330 UT on 21th January 2016 until 0700 UT on 22th January 2016, showing the atypical strong Es layers.

Similar strong Es layers were observed in BV ionograms during the recovery phase of all the magnetic storms shown in Table 1. We have selected the moderate/intense magnetic storms (Dst < -50) that occurred in 2016 and 2017, a period in which we had data available for the BV region. Notice that all density increases occurred during the magnetic storm recovery phase. As it will be discussed later, these layers cannot be formed by wind shear mechanism only, since the

tidal winds in the regions near the geographic equator, as BV, have small amplitudes in their meridional and zonal component (Figure 1). Therefore, another mechanism must be acting at this region to form these strong layers.

Table 1: List of strong Es layer in BV associated to moderate/intense magnetic storms (Dst < -50) in 2016 and 2017.

Arrival of the CME on Earth	Minimum Dst (nT)	Beginning of the strong Es layer observation	Magnetic Storm Phase of Es layer observation
05 March 2016; 1900UT	-98	06 March 2016; 2140 UT	Recovery
13 October 2016; 0600UT	-104	14 October 2016; 2350UT	Recovery
04 November 2016; 1800UT	-50	04 November 2016; 2350 UT	Recovery
10 November 2016; 0000UT	-59	12 November 2016; 2000 UT	Recovery
27 May 2017; 2200UT	-125	30 May 2017; 2050 UT	Recovery
16 July 2017 1500UT	-72	17 July 2017 2310 UT	Recovery

In face of such observation at BV, we looked for strong Es layers in the same data collected in other regions aiming to define the geographical/geomagnetical extent of such phenomena. Figure 4 shows the *fb*Es (green line) and *ft*Es (orange line) parameters between 21 and 23 January 2016 for four different low latitude regions in Brazil, BV, CG, FLZ, and SLZ. The FLZ and SLZ are regions close to the magnetic equator, whereas CG is located at the same magnetic meridian as BV, but in the Southern Hemisphere. From this figure, it is clear that the high top frequency values of the Es layer, i.e. the higher electron density, were only observed in BV. For the FLZ and SLZ regions, the *ft*Es/*fb*Es during the nighttime had low values, and it disappeared in few hours.

Once we have no wind measurements in these regions (SLZ and FLZ), associated with the GSWM-00 output showing not enough wind shears to form Es layers, the Es layer modeling at the Brazilian regions faces some difficulties. Nevertheless, we recall that *Resende et al. [2017b]* studied the wind behavior to form Es layers using an all-sky interferometric meteor radar installed in São João do Cariri (7.23S, 36.32W, dip: -22.16), the nearest region to São Luís. They observed that the Es layer electron density in São Luís has low values during the day, disappearing in the night hours. This behavior agrees with the observations on SLZ and FLZ in the analyzed period here. The authors concluded that the zonal wind component was found to be the most important for the Es layer formation, and this component at a nearby equator station has low amplitudes forming weak Es layers. Furthermore, in some hours for these regions, the *fb*Es shows a typical behavior characterized by an enhancement during the morning period, starting about 09 UT (06 LT), and reaching maxima values about 15 UT (12 LT), followed by a steady decrease, reaching the quiescent values after 21 UT (18 LT) [*Resende et al., 2017a*]. For all these reasons, the Es layers in SLZ and FLZ do not have any atypical behavior as in BV.

Regarding CG (panel b), the Es layer completely disappeared at the moment of the occurrence of the strong Es layers in BV. In fact, the CG is located at the same magnetic meridian as BV, meaning that the integrated field line conductivity is the same in both these regions [*Abdu et al., 2009a*]. *Batista et al. [2008]* studied the relation between the spread F (SF) occurrence and Es layer characteristics using simultaneous data to look for any possible relation between these two phenomena in BV, CG, and Cachimbo (9.8S, 54.5W). Several instruments

were provisionally installed in these stations during the Conjugate Point Equatorial Experiment (COPEX) campaign, which occurred in Brazil from October to December 2002. They did not detect any significant correlation between the SF occurrence/generation at the magnetic equator and the presence of Es layers at the conjugate E regions along the same field line. However, they observed that the Es layers were stronger in BV when compared to those detected in CG. Nevertheless, they did not study the effect of the vertical equatorial electric field (that is associated with the eastward electric field pre-reversal enhancement) with the Es development or disruption.

Lastly, the digisonde installed recently in BV allows the analysis of the recurrent atypical Es layer during the recovery phase of the magnetic storm. In this context, we performed a deeper analysis of the magnetic storm period in January 2016 to find a possible explanation of such behavior in BV.

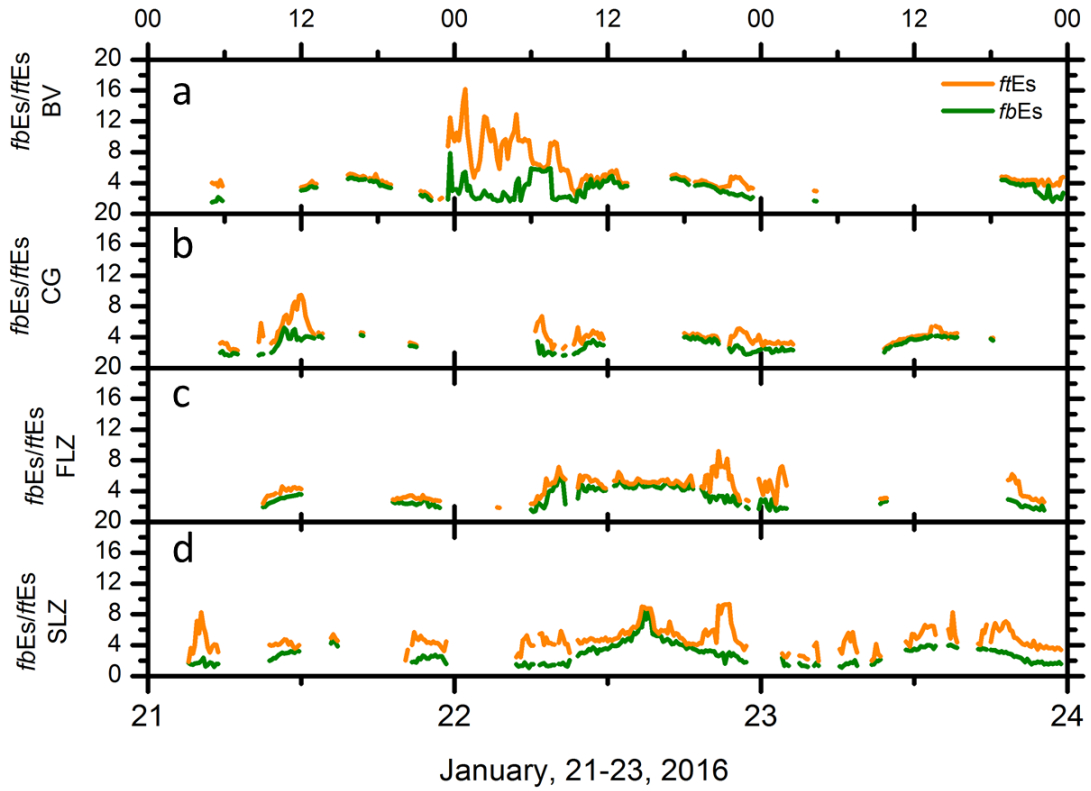

Figure 4. The *fb*Es and *ft*Es parameters at four Brazilian: low latitudes, Boa Vista (panel a), Campo Grande (panel b), and equatorial regions, Fortaleza (panel c), São Luís (panel d) on 21-23 January 2016.

3.3 The F region effect

Figure 5a presents the F2 layer peak height (*hm*F2) parameter for 21 and 22 January 2016 over BV. The blue line refers to a quiet day (January 18) used as reference. An important characteristic observed in this Figure is that the F layer peak height enhancement near sunset (hachured area) was reduced in relation to the quiet period. The possible causes for this *hm*F2

reduction can be either 1) a northward meridional wind which contributes to the lowering of the layer, 2) a reduction of the eastward electric field through an overshielding effect of a PPEF or 3) a westward disturbance dynamo electric field (DDEF). In the present case it seems that the meridional wind is directed southward as we can see in Figure 5b. This Figure presents the difference between *hm*F2 measured at CG and BV (d*hm*F2 = $hmF2_{CG}$ – $hmF2_{BV}$), which, as discussed in *Abdu et al. [2009a]* and in *Batista et al. [2017]*, is a measure of the interhemispheric symmetry/asymmetry in *hm*F2. Positive/negative values of d*hm*F2 indicate transequatorial meridional wind (TMW) directed northward/southward. As it can be seen from Figure 5b, at the time of the *hm*F2 reduction over BV, d*hm*F2 is negative, indicating a southward TMW. Such a TMW would contribute to increase the F layer height over BV which is not observed in the data. The second hypothesis of an overshielding PPEF would occur under the presence of northward turning of the IMF-B_z, which was not observed during the time interval under consideration. In fact, B_z is close to zero and AE presents minor fluctuations (see Figure 2). Therefore, it seems that a westward disturbance dynamo electric fields (DDEF) is the most probable candidate to explain the reduction in the rise of F layer peak height during the time of interest for this study.

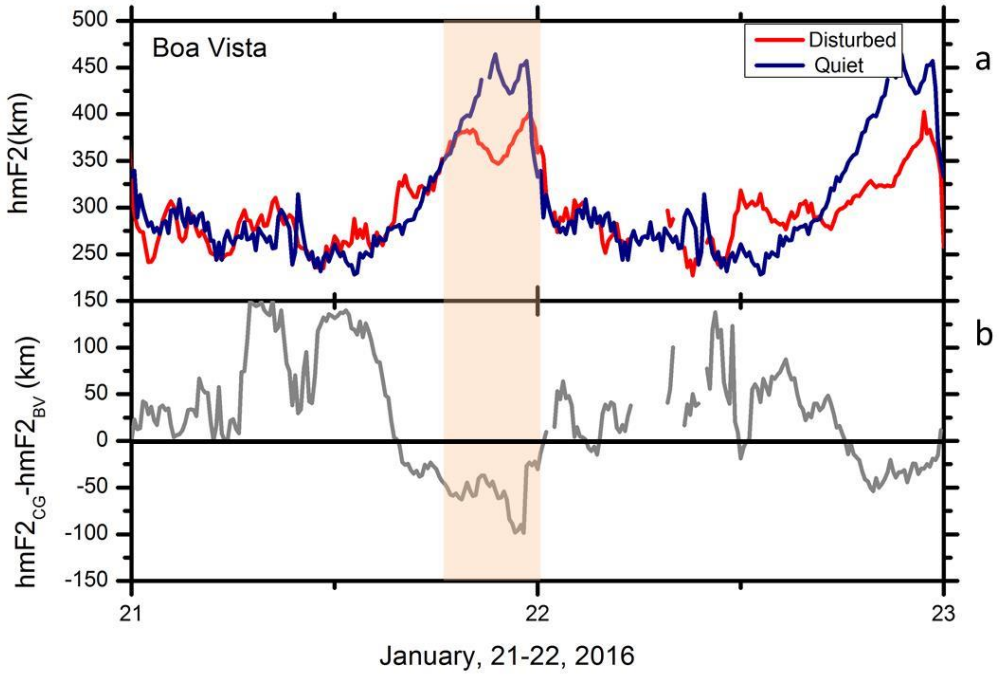

Figure 5. The *hm*F2 parameter at Boa Vista (panel a) and the difference between hmF2 in Campo Grande and Boa Vista (panel b) on 21-23 January 2016.

To confirm the DDEF effect in the F-layer height, we calculated the ExB drift during the hours when the strong Es layers were observed. In order to perform this calculation, it is important to have in mind that the vertical drift velocity using the relation mentioned before ($\Delta hF/\Delta t$) is valid near sunset and night hours when the F-layer height is equal or higher than 300

km. If the layer is below this height, then the recombination processes need to be taken into account for the drift velocity calculation. Thus, the vertical drift velocity is given by

$$V_{BV} = V_{ap} - \beta H, \quad (1)$$

where the V_{BV} refers to the drift velocity at Boa Vista (BV), V_{ap} is the apparent vertical drift (measured) for a station, β is the recombination coefficient, and H is the scale height of ionization. The recombination coefficient is given by

$$\beta = k_1[N_2] + k_2[O_2]. \quad (2)$$

The reaction coefficients $k_1$and k_2 can be found in *Nogueira et al. [2011]*, and $[N_2]$ and $[O_2]$ are the neutral molecular nitrogen and oxygen number densities, respectively, which were obtained from the atmospheric model MSISE-90 *[Hedin et al., 1991]*.

Additionally, for stations located outside the magnetic equator, like BV, we need to consider the meridional wind since this component may contribute to the vertical plasma motion as well [*Rishbeth et al., 1978; Nogueira et al., 2011*]. Therefore, V_{ap} is given by:

$$V_{ap} = V_D\, cosI \pm U_F cosIsenI - w_D sin^2 I, \quad (3)$$

where V_D is the vertical drift velocity calculated as $\Delta h/\Delta t$, I is the magnetic inclination angle (~18° in BV), U_F is the meridional wind in the F region (positive northward), w_D is the contribution to the vertical plasma velocity due to diffusion given by $w_D = g/\nu_i$, where g is the acceleration of gravity, and the ν_i is the ion-neutral collision frequency. We used the same methodology described in *Nogueira et al. [2011]*, in which ν_i is computed as:

$$\nu_i = 4.34 \times 10^{-16}[N_2] + 4.28 \times 10^{-16}[O_2] + 2.44 \times 10^{-16}[O], \quad (4)$$

where $[N_2]$, $[O_2]$, and $[O]$ were obtained from MSISE-90.

The vertical drift calculated according to the above equation is shown in Figure 6. The grey line in the Figure refers to the quiet period drift whereas the orange line refers to the recovery phase of the magnetic storm that we call disturbed period. Positive/negative drift values are directed to the east/west. Notice that the DDEF effect can be clearly seen, since, during the PRE hours (2100 UT), the ExB drift was inhibited, presenting opposite direction of the typical quiet time behavior. After these hours, the drift velocity tried to recovery and reached values higher than the quiet drift velocity. Finally, after 0200 UT, the drift velocity presented an oscillatory behavior, showing that the drift was returning to its typical values.

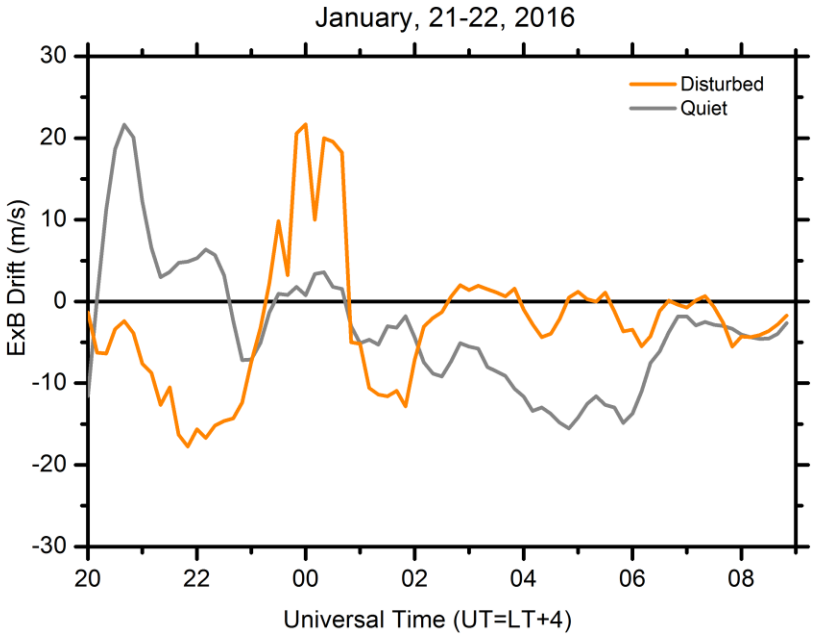

Figure 6. The ExB drift in quiet (grey line) and disturbed (orange line) periods between the 2000 UT and 0900 UT at Boa Vista on 21-22 January 2016.

Generally, the DDEF show low values of downward disturbance drifts between 0700 and 1700 LT, followed by larger downward drifts near sunset and upward drift near midnight. The local time and seasonal dependence of the disturbance dynamo drifts are largely anti-correlated with those of the prompt penetration drifts or quiet time drift [*Fejer et al., 2008*], which seems to be in agreement with the results presented in Figure 6. We also analyzed the equatorial ionization anomaly (EIA) modification using TEC Maps over South America to observe and confirm the presence of the DDEF effect. Figure 7 shows the TEC over South America. The solid black line across the map indicates the magnetic equator location in 2016. In Figure 7a we have the TEC Map during the reference quiet day (18 January 2016). Notice that the EIA crests are well demarked at low latitude stations (yellow colors in maps) between 2100 UT and 2300 UT, which is the typical behavior of the ionosphere plasma over Brazil. On 21 January 2016, it is possible to observe a clear weakening of the EIA crest near sunset time (Figure 7b). Similar behavior was observed in a study by *Nogueira et al. [2011]*, in which they analyzed the response of the ionosphere during two magnetic storms that occurred in 2001. In fact, they analyzed the EIA intensity and the variations in the zonal electric field in different phases of the magnetic storms. They found that the PPEF mechanism occurred during the main phase in both cases, causing an enhancement in the EIA. However, during the recovery phase, they found that the DDEF almost caused an EIA crest disappearance, agreeing with our results.

We emphasize here that this mechanism is a global phenomenon. Thus, the westward electric field in PRE hours due to disturbance dynamo occurs in all regions of Brazil, being more visible in those near the magnetic equator.

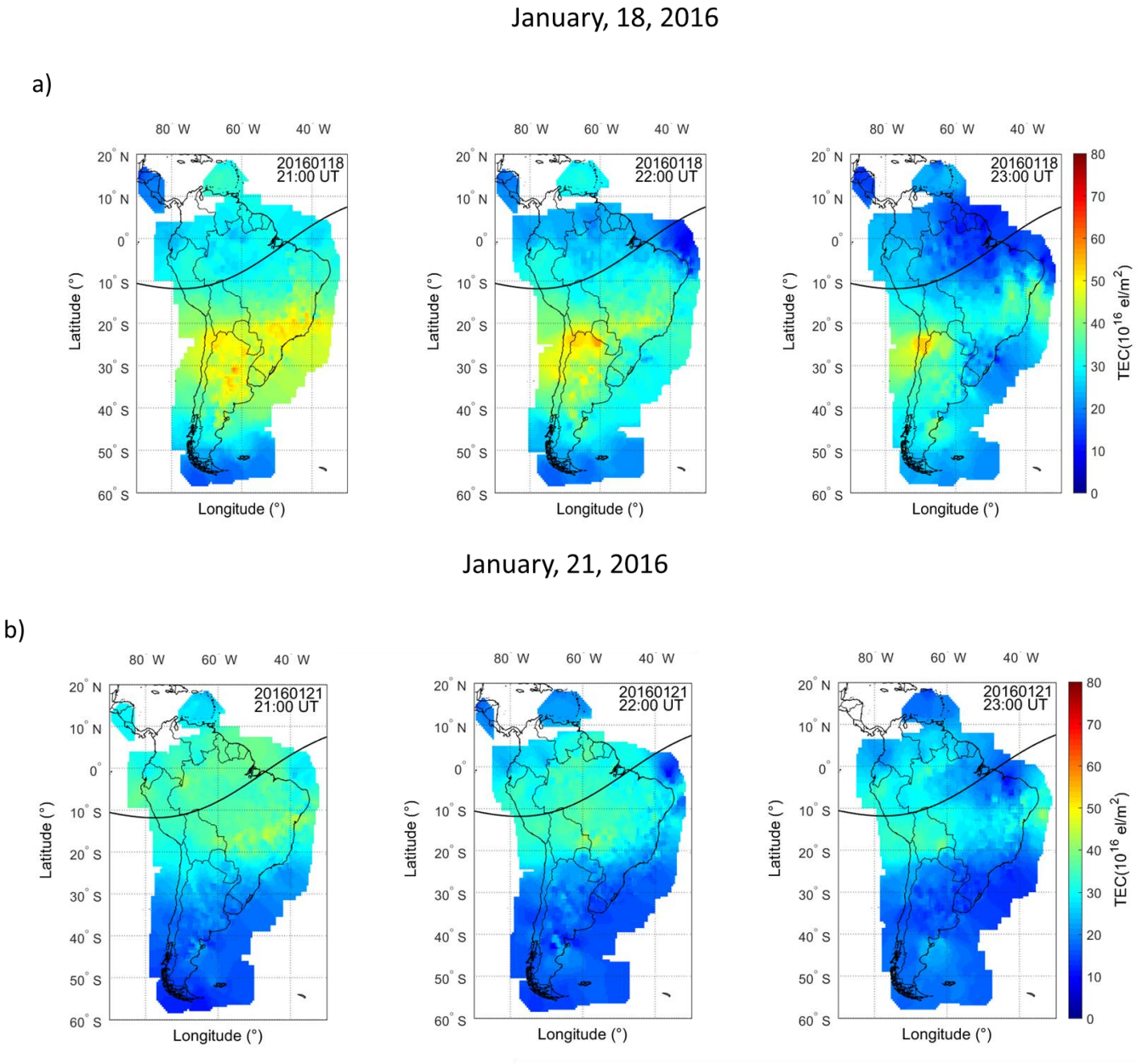

Figure 7. Longitude versus latitude distribution of the TEC Map over South America at one hour interval during (a) the quiet time period, and (b) covering the period of the disturbance dynamo effect.

Therefore, the inhibition of the PRE drift and EIA are concrete evidences of the influence of a DDEF that occurred in the recovery phase of the 20 January magnetic storm, as already discussed by several authors [*Sastri et al., 1988; Abdu et al, 1997; Abdu et al., 2006; Santos et al., 2012*]. Thus, we believed that the strong Es layer formation on BV can be influenced by the DDEF. This fact was analyzed in detail and it is shown hereafter.

3.3. Analysis of the electric field effect using simulations

In this work we are pointing out that the only possible mechanism to form the strong Es layers in BV is due to an electric field superposed to the wind shear mechanism. According to *Fejer and Scherliess [1995]* the relationship between the zonal electric field and the vertical drift produced by this electric field is approximately 1 mV/m to 40 m/s. Analyzing Figure 6, the drift during the hours of the PRE was approximately -20 m/s, which corresponds to a westward electric field of 0.5 mV/m. Comparing with the ionograms in Figure 2, the strong Es layer starts to occur at 2330 UT, shortly after the electric field reached its highest value. After, the Es layer tries to return to normal conditions, around 0130 UT, when the *fb*Es and *ft*Es reached the lowest values in this period. At the same time, the drift velocity on January 22, 2016 showed a positive value of ~15 m/s, meaning an eastward electric field of approximately 0.42 mV/m. However, at 0200 UT, the drift velocity became negative, meaning that the zonal electric field is westward again. At 0230 UT, the *ft*Es reached values higher than 15 MHz, but this behavior did not last long since the vertical drift oscillated in the next hours. Thus, this result shows a possible connection between the westward electric field and the Es layers formation.

We included the electric field values in MIRE to verify this behavior. First, we included a constant westward electric field equal to 0.5 mV/m between 2000 UT and 0600 UT that corresponds to the PRE vertical drift of -20 m/s. Figure 8 show Height-Time (HT) Maps of the electron density profile simulated by MIRE (color scale) over BV on January 22, 2016. The background color maps show a typical behavior of the E region electron density, with low values in the night period and expressive electron density in the daytime. In Figure 8a, we considered only the wind effect obtained by the GSWM-00. Notice that MIRE successfully simulated the Es layers, which are observed as the thin descending layers in some hours. The Es layers were formed around 110 km with low density and a downward movement is observed, agreeing with the theory about the Es layer behavior [*Bishop and Earcle, 2003; Haldoupis et al., 2006*]. This scenario is typical for Es layers formed by the wind shear mechanism [*Resende et al., 2017b*]. Furthermore, notice that the Es layer did not seem to occur during the daytime since its density was very close to the background E region density. However, in the nighttime, which is our interest in this study, the Es layers were clearly observed.

Figure 8b shows the HT Maps of electron density profile simulated by MIRE with the selected constant value for the electric field. It is possible to observe that the Es layer during the night hours were stronger when it was compared with Figure 8a. From 18 UT, the density layer increased significantly, approximately 1.5 times more. During the first hours of the morning (0000 UT until 0400 UT), the Es layer density when considering the electric field reached almost 10^5 electrons/cm^3, whereas the Es layer formed only by the winds reached a density of approximately 10^4 electrons/cm^3. Therefore, the constant westward electric field caused a strengthen to these Es layers in BV.

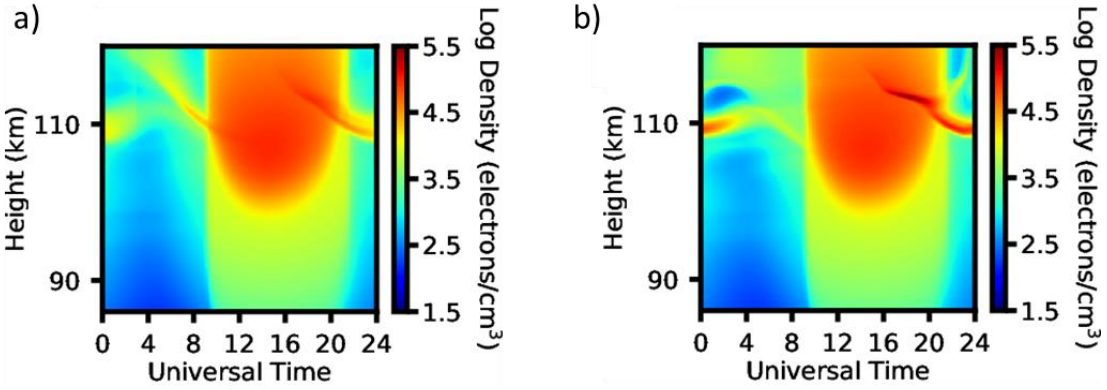

Figure 8. Electron density as a function of Universal Time (UT) and height (km) simulated by MIRE considering the diurnal and semidiurnal tidal winds representative of January 2016 (a) and considering the westward zonal electric field component of 0.5 mV/m (b).

It is possible to notice in Figure 8b that the constant electric field included during the nighttime in MIRE caused modifications to the Es layer profile. *Resende et al. [2016]* and *Moro et al. [2017]* showed that the zonal electric field can cause a modulation in the existing Es layers, which is still attributed to the tidal wind mechanism. They studied the equatorial regions electric field due to the EEJ current to analyze the Es layer formation, concluding that the zonal electric fields are not efficient enough to create or disrupt any Es layers. The only observable effect is some modulation. Therefore, in our case, it was possible to confirm that the electric field caused some influence in diurnal times.

Carrasco et al. [2007] analyzed the vertical electric field influence in the Es layers during the F region pre-reversal enhancement (PRE) in the zonal electric fields by mapping these electric fields through the equipotential magnetic field lines. Depending on the direction of the vertical electric field component, they observed an Es layer disruption or enhancement around the sunset and its correlation with the PRE. In fact, a vertical electric field during the sunset can be mapped to low latitudes regions, causing some influence in the Es layers. On the other hand, *Abdu et al. [2014]* investigated the same situation of low-latitude Es layers during the magnetic storm periods. They show that a PPEF of an overshielding electric field with the westward polarity in the evening sector can cause the sporadic E layers formation near 100 km. The deeper analysis performed by them concluded that the ionization of the Es layer formation is driven by the enhanced ratio of field line integrated Hall to Pedersen conductivity ($\sum$H)/($\sum$P) during the magnetic storms, influencing the electric field components in F region. After, the vertical electric field is mapped to E region, which can form strong Es layers. To confirm the enhancement in the $\sum$H/$\sum$P ratio, they used the energetic particle precipitation since the regions analyzed are located in the South Atlantic Magnetic Anomaly (SAMA). Therefore, they concluded that during the disturbed periods the electric field effects on Es layers occur more in the SAMA region.

In our study, it was not possible to analyze the influence of the F region vertical electric field mapped to BV, since we do not have measurements in equatorial regions for the same magnetic field line. In fact, this is a possible mechanism due to the absence of the Es layers in CG. The vertical electric field can be mapped to BV and CG, in opposite directions, causing a strengthening and disruption of Es layers, respectively. However, the explanation in *Abdu et al*.

[2014] about the enhancement in the ∑H/∑P ratio in SAMA regions is not possible since BV is located far from the northern border of the anomaly.

The literature [*Fürst et al., 2009; Ginet et al., 2007*] shows that the BV region is located on the Northwest boundary of the SAMA, which means that this region may receive few influences of the particle precipitation. *Da Silva et al. [2016]*, presented the preferential particle precipitation region on the SAMA through the distribution of the X-Ray (3.0–31.5 keV energy range) of the upper atmosphere measured by RPS (X-ray spectrometer) device on board of the CORONAS-F satellite, in which it is clearly seen that there is no particle precipitation over BV. Even knowing that there is little chance of the charged particle precipitation in the region of the interest, it is extremely important to investigate the dynamic processes on the outer radiation belt during the specific case study (2200 - 0000 UT on January 22, 2016), as following below.

The Van Allen Probes data [*Mauk et al., 2012*] showed that the outer radiation belt flux (high-energy, Figure not shown) for this event is considerable stable (without dropout and/or enhancement). The data also showed the absence of the Chorus (from hundreds of Hz up to about 10 kHz) and Electromagnetic Ion Cyclotron – EMIC (0.3 Hz up to 3 Hz) wave activities, it means the pitch angle scattering mechanism [*Kennel and Petschek, 1966; Thorne et al., 2010*] did not occur, consequently charged particles were not launched in the loss cone, resulting to not occurrence the particle precipitation during all period of this case study. Through this investigation may suggest that the Es layers detected here are generated without the influence of the particle precipitation. Therefore, it is concluded that the ∑H/∑P enhancement which is directly intensified in the SAMA region during the magnetic storms has little or no influence on the mechanisms able to intensify the Es layers on BV region.

Another possibility is the direct effect of the DDEF in BV. In fact, the westward electric field can intensify the Es layers as shown in *Abdu et al. [2014]*. Indeed, the fast variation of the electric field from eastward to westward on the night of 21-21 January 2016 may be causing the oscillations in the frequency parameters observed in Figure 3. We believe that the zonal electric field around 0.5 mV/m-1mV/m may have driven plasma densification as proposed by *Dagar et al. [1977]*. In their analysis, the values of the zonal component of the electric field, even with winds influence, could form Es layers when their values were smaller than 2 mV/m. Also, *Dagar et al. [1977]* found that the zonal electric field component increases the Es layer electron density, and, even if the electric field ceases, it still takes time for the Es layer to disappear completely.

Therefore, we analyzed the evolution of the electric fields obtained by the vertical drift of Figure 6. For each value between 2000 UT and 0000 UT, and from 0000 UT to 0600 UT, we calculated the electric field using the relationship in *Fejer and Scherliess [1995]*. Thus, the electric field that was included in MIRE has the behavior presented in Figure 9a, in which the negative and positive values mean the westward and eastward polarity, respectively. In Figure 9b we show the simulation results, in which it is possible to verify that the Es layer is strong during almost the entire day. In some hours during the daytime, the Es disappear. However, our focus is around the nighttime period. Also, the Es layer seems to be weakened around 0400 UT to 0600 UT, but right after it becomes stronger again. This result shows that the inhibition of the PRE due to the action of the disturbance dynamo electric field can influence the enhancement of Es layer in our simulations. We believe that this behavior did not occur in CG because the vertical drift was smaller and the electric field was not enough to strengthen the Es layers. Furthermore, the tidal wind configuration in CG is completely different with respect to BV, which may also

have influenced the absence of the Es layers. In fact, the GSWM-00 is not effective in forming Es layers far away from the geographical equator [*Resende et al., 2017a*], precluding a deeper analysis for this region.

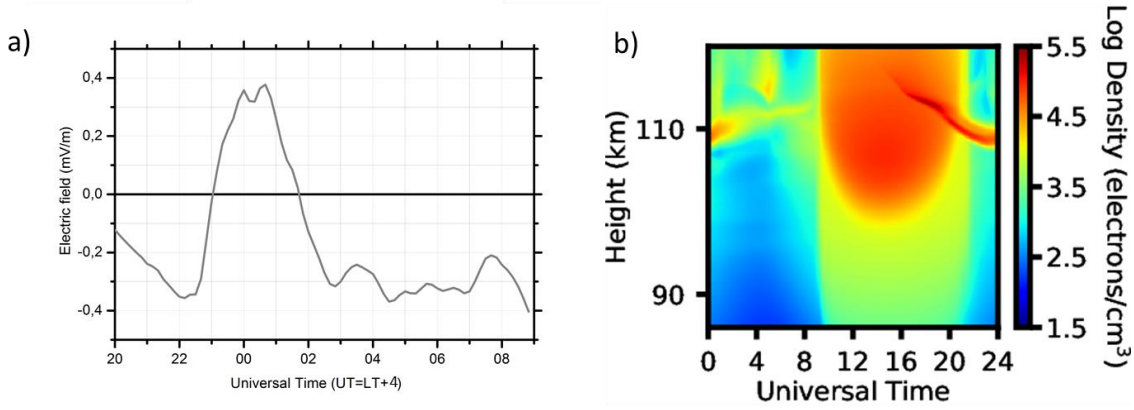

Figure 9. Zonal electric profile between 20 UT and 09 UT on the 21-22 January 2016 (a), and the electron density as a function of Universal Time (UT) and height (km) simulated by MIRE considering the winds and the zonal electric field (b) on BV.

Finally, although there is evidence that the direct DDEF may be influencing the Es layers intensification in BV, the proposal of *Abdu et al. [2014]* cannot be totally discarded. Even BV been outside the SAMA region, the vertical electric fields mapped from equatorial F region to low latitudes can have some influence on the Es layers formation in BV. However, the Es layers in BV appear to be stronger than those observed in the study of *Abdu et al. [2014]*. Besides that, the zonal electric field values used in the previous analysis of the Es layer [*Dagar et al., 1977*] are similar to those of our study, corroborating that the intensifications observed may be associated with DDEF. Furthermore, using simulations for the first time, it was possible to verify that these strong layers in BV are due to the combined effect of these electric fields with the winds. Lastly, it is noteworthy that the influence of the electric fields in the Es layers is a particularity of regions such as Brazil, which has the magnetic equator crossing the country from west to east.

4 Conclusions

We have performed in this work a comprehensive analysis of the strong Es layer formation over Boa Vista (BV). These layers are been observed during the recovery phase of the magnetic storms. Therefore, we used the TEC and digisonde data, as well as modeling results to provide some explanation of this behavior.

We investigated in detail the ionospheric response to the disturbing electric fields in these atypical Es layers appearance during the magnetic storm of 21-22 January 2016. Our finds reveal that the possible mechanism to form these strong Es layers in BV is due to a disturbed electric field caused by the disturbance dynamo. We performed a deep study around this magnetic storm, and the results show that the Es layer intensification is related to the F-region pre-reversal enhancement inhibition of the vertical drift. This was caused by a westward electric field during

the disturbance dynamo effect. Furthermore, we confirmed the disturbance dynamo occurrence using the TEC Maps over South America, which showed the weakness of the equatorial ionization anomaly crest.

After that, we quantified the electric field influence using MIRE model including the winds obtained by the GSWM-00. In fact, the wind shear mechanism is the main agent to form a weak Es layer in BV. We believe that the disturbed electric field due to the disturbance dynamo was superposed to the wind shear mechanism, forming these strong Es layers. Thus, we used the relationship between the zonal electric field and the vertical drift to obtain the electric field values to simulate Es layers in MIRE. The results show that a constant westward electric field equal to 0.5 mV/m or an evolution of the electric fields obtained by the vertical drift along the day caused a significant Es layer electron density enhancement in simulations. This behavior occurred only when the disturbance dynamo was effective.

Additionally, we analyzed the other possible causes of such strong Es layers that are occurring in BV to confirm that the disturbance dynamo electric field is the main formation agent of these Es layer. We verify that the enhancement in the $\sum H/\sum P$ ratio can be a possible mechanism to form denser Es layers. However, this enhancement occurs in regions near of the South Atlantic Magnetic Anomaly, which can have energetic particle precipitation. Therefore, in Boa Vista this mechanism is not effective since this region is located far from the northern border of the anomaly.

Finally, the combined results from the model and observational data confirmed that these atypical Es layers are due of the disturbance dynamo electric field. Thus, it is noteworthy that the influence of the electric fields in the Es layers is a particularity of regions such as Brazil, which has the magnetic equator crossing the country from west to east.

Acknowledgments, Samples, and Data

L. C. A. Resende would like to thank the China-Brazil Joint Laboratory for Space Weather (CBJLSW), National Space Science Center (NSSC), Chinese Academy of Sciences (CAS) for supporting her postdoctoral. S. Jiankui would like to thank the National Natural Science Foundation of China (grant 41674145). C. M. Denardini thanks CNPq/MCTI, grant 03121/2014-9. I. S. Batista thanks CNPq/MCTI, grants 405555/2018-0 and 302920/2014-5. V. F. Andrioli would like to thank the CBJLSW/NSSC/CAS for supporting her postdoctoral. J. Moro would like to thank the CBJLSW/NSSC/CAS for supporting his postdoctoral, and the CNPq/MCTIC (grant 429517/2018-01). L. Silva would like to thank the CBJLSW/NSSC/CAS for supporting her postdoctoral. P. F. Barbosa Neto thanks Capes/MEC (Grant 1622967). The authors thank the High Altitude Observatory (HAO) of the National Center for Atmospheric Research (NCAR), in Colorado (http://web.hao.ucar.edu/public/research/tiso/gswm/gswm.html) for providing wind data used in MIRE model. The authors thank the OMNIWEB (https://omniweb.gsfc.nasa.gov/form/dx1.html) for providing B_z, V_{sw}, AE and Dst parameters used in the classification of the days. The Digisonde data from Boa Vista and TEC data can be downloaded upon registration at the Embrace webpage from INPE Space Weather Program in the following link: http://www2.inpe.br/climaespacial/portal/en/.

603 **References**

604

605 Abdu, M. A., I. S. Batista, P. Muralikrishna, J. H. A. Sobral (1996). Long term trends in sporadic
606 E layers and electric fields over Fortaleza, Brazil. *Geophysical Research Letters*, 23(7), 757-
607 760, doi:10.1029/96GL00589.

608 Abdu, M. A. (1997). Major phenomena of the equatorial ionosphere- thermosphere system under
609 disturbed conditions. *Journal of Atmospheric and Terrestrial Physics*, 59, 1505-1519,
610 doi:10.1016/S1364-6826(96)00152-6.

611 Abdu, M. A., J. R. de Souza, J. H. A. Sobral, and I. S. Batista (2006). Magnetic storm associated
612 disturbance dynamo effects in the low and equatorial latitude ionosphere, in Recurrent
613 Magnetic Storms: Corotating Solar Wind Streams. *Geophysical Monograph Series*, 167,
614 283-304, doi:10.1029/167GM22.

615 Abdu, M. A., Batista, I. S., Reinisch, B. W., de Souza, J. R., Sobral, J. H. A., Pedersen, T. R.,
616 Groves, K. M. (2009a). Conjugate Point Equatorial Experiment (COPEX) campaign in
617 Brazil: Electrodynamics highlights on spread development conditions and day-to-day
618 variability. *Journal of Geophysical Research: Space Physics*, 114(A4), 1-21.
619 doi:10.1029/2008ja013749.

620 Abdu, M. A., G. M. Brum. (2009b). Electrodynamics of the vertical coupling processes in the
621 atmosphere-ionosphere system of the low latitude region. *Earth, Planets Space*, 61, 385-395,
622 doi: 10.1186/BF03353156.

623 Abdu, M. A., J. R. de Souza, I. S., Batista, M. A. Santos, J. H. A. Sobral, R. G. Rastogi, H.
624 Chandra (2014). The role of electric fields in sporadic E layer formation over low
625 latitudes under quiet and magnetic storm conditions. *Journal of Atmospheric and*
626 *Terrestrial Physics*, 115, 95-105, doi: 10.1016/j.jastp.2013.12.003.

627 Balan, N., Alleyne, H., Walker, S., Reme, H., McCrea, I., Aylward, A. (2008). Magnetosphere-
628 ionosphere coupling during the CME events of 07–12 November 2004. *Journal of*
629 *Atmospheric and Terrestrial Physics*, 70(17), 2101–2111,
630 doi:10.1016/j.jastp.2008.03.015

631 Batista, I. S., Abdu, M. A., Carrasco, A. J., Reinisch, B. W., de Paula, E. R., Schuch, N. J.,
632 Bertoni, F. (2008). Equatorial spread F and sporadic E-layer connections during the
633 Brazilian Conjugate Point Equatorial Experiment (COPEX). *Journal of Atmospheric and*
634 *Solar-Terrestrial Physics*, 70(8-9), 1133–1143, doi:10.1016/j.jastp.2008.01.007.

635 Batista, I. S., Candido, C. M. N., Souza, J. R., Abdu, M. A., de Araujo, R. C., Resende, L. C. A.
636 Santos, A. M. (2017). F3 layer development during quiet and disturbed periods as
637 observed at conjugate locations in Brazil: The role of the meridional wind. *Journal of*
638 *Geophysical Research: Space Physics*, 122, 2361-2373, doi:10.1002/2016JA023724.

639 Bishop, R. L., Earcle, G. D. (2003). Metallic ion transport associated with midlatitude
640 intermediate layer development. *Journal of Geophysical Research: Space Physics*, 108
641 (A1), 10-19. http:// dx.doi.org/10.1029/2002JA009411.

642 Blanc, M., Richmond, A. D. (1980). The ionospheric disturbance dynamo. *Journal of*
643 *Geophysical Research: Space Physics*, 85(A4), 1669–1686.
644 doi:10.1029/JA085iA04p01669.

645 Buriti, R. A., Hocking, W. K., Batista, P. P., Medeiros, A. F. (2008). Observations of equatorial
646 mesospheric winds over Cariri (7.4° S) by a meteor radar and comparison with existing
647 models. *Annales Geophysicae*, 26, 485-497, doi: 10.5194/angeo-26-485-2008.

648 Carrasco, A. J., Batista, I. S., Abdu M. A. (2007). Simulation of the sporadic E layer response to
649 pre-reversal associated evening vertical electric field enhancement near dip equator.
650 *Journal of Geophysical Research: Space Physics*, 112(A06):324-335,
651 doi:10.1029/2006JA012143.

652 Dagar, R., P. Verma, O. Napgal, C. S. G. K. Setty (1977), The relative effects of electric fields
653 and neutral winds on the formation of the equatorial sporadic layers. *Annales*
654 *Geophysicae*, 33(3), 333–340.

655 Da Silva, L. A., Satyamurty, P., Alves, L. R., Souza, V. M., Jauer, P. R., Silveira, M. V. D.,
656 Vieira, L. E. A. (2016). Comparison of geophysical patterns in the southern hemisphere
657 mid-latitude region. *Advances in Space Research*, 58(10), 2090–2103,
658 doi:10.1016/j.asr.2016.04.003.

659 Denardini, C. M., Dasso, S., Gonzalez-Esparza, J. A. (2016). Review on space weather in Latin America.
660 2. The research networks ready for space weather. *Advances in Space Research*, 58(10), 1940–1959.
661 https://doi.org/10.1016/j.asr.2016.03.013

662

663 Fürst, F., Wilms, J., Rothschild, R. E., Pottschmidt, K., Smith, D. M., and Lingenfelter, R.(2009).
664 Temporal variations of strength and location of the South Atlantic Anomaly as measured
665 by RXTE. *Earth Planet Science Letters*, 281, 125–133, doi:10.1016/j.epsl.2009.02.004.

666 Ginet, G. P., Madden, D., Dichter, B. K., and Brautigam G, D. H. (2007). Energetic proton maps
667 for the South Atlantic Anomaly. *IEEE Radiation Effects Data Workshop*, Honolulu, HI,
668 USA, 23–27 July 2007, 1–8.

669 Gonzalez, W.D., Joselyn, J.A., Kamide, Y., Kroehl, H.W., Rostoker, G., Tsurutani, B.T.,
670 Vasyliunas, V.M. (1994). What is a magnetic storm? *Journal of Geophysical Research:*
671 *Space Physics*, 99 (A4), 5771-5792, doi: doi.org/10.1029/93JA02867.

672 Hagan, M. E., Forbes, J. M. (2002). Migrating and nonmigrating diurnal tides in the middle and
673 upper atmosphere excited by tropospheric latent heat release. *Journal of Geophysical*
674 *Research: Space Physics*, 107(D24), 4754, doi:10.1029/2001JD001236.

675 Hagan, M. E., Forbes, J. M. (2003). Migrating and nonmigrating semidiurnal tides in the upper
676 atmosphere excited by tropospheric latent heat release. *Journal of Geophysical Research:*
677 *Space Physics*, 108(A2), 1062, doi:10.1029/2002JA009466.

678 Haldoupis, C., Meek, C., Christakis, N., Pancheva, D., Bourdillon, A. (2006). Ionogram height-
679 time intensity observations of descending sporadic E layers at mid-latitude. *Journal of*

Atmospheric and Terrestrial Physics, 68 (539), 539–557, doi:10.1016/ j.jastp.2005.03.020.

Haldoupis, C. (2011). A tutorial review on Sporadic E layers, Aeronomy of the Earth's Atmosphere-Ionosphere. *IAGA Book Series*, 29 (2), 381-394, doi: 10.1007/978-94-007-0326-1_29.

Hedin, A. E., Biondi, M. A., Burnside, R. G., Hernadez, G., Johson, R. M., Killen, T. L., Mazaudier, C., Meriwether, J. W., Salah, J. E., Sica, R. J., Smith, R. W., Spencer, N. W., Wickwar, V. B., Virdi, T. S. (1991). Revised global model of thermosphere winds using a satellite and ground-based observations. *Journal of Geophysical Research: Space Physics*, 96(A5), 7657–7688, doi: 10.1029/91JA00251.

Fejer, B. G., Scherliess,L. (1995). Time dependent response of equatorial ionospheric electric fields to magnetospheric disturbances. *Geophysical Research Letters*, 22, 851-854, doi: 10.1029/95gl00390.

Fejer, B. G. (1997). The electrodynamics of the low-latitude ionosphere: Recent results and future challenges. *Journal of Atmospheric and Terrestrial Physics*, 59, 1465–1482, doi: 10.1016/S1364-6826(96)00149-6.

Fejer B. G., Jensen J. W., Su S. Y. (2008). Seasonal and longitudinal dependence of equatorial disturbance vertical plasma drifts *Geophysical Research Letters*, 35(L20106):2008G, doi:10.1029/L035584.

Kelley, M. C., Makela, J. J., Chau, J. L., Nicolls, M. J. (2003), Penetration of the solar wind electric field into the magnetosphere/ionosphere system. *Geophysical Research Letter*, 30(4), 1158, doi:10.1029/2002GL016321.

Kennel, C. F. and H. E. Petschek. (1966). Limit on stably trapped particle fluxes. Journal Geophys. Reseach. https://doi.org/10.1029/JZ071i001p00001

Kopp, E. (1997), On the abundance of metal ions in the lower ionosphere. *Journal of Geophysical Research: Space Physics*, 102, 9667- 9674, doi: 0148-0227/97/97JA-003845.

Mauk, B. H., N. J. Fox, S. G. Kanekal, R. L. Kessel, D. G. Sibeck, and A. Ukhorskiy. (2012). Science objectives and rationale for the radiation belt storm probes mission. *Space Science Review*, 179, 3–27, doi:10.1007/s11214-012-9908-y.

Mathews, J. D. (1998). Sporadic E: current views and recent progress. *Journal of Atmospheric and Terrestrial Physics*, 60, 413-435, doi: 10.1016/S1364-6826(97)00043-6.

Moro, J., L. C. A. Resende, C. M. Denardini, J. Xu, I. S. Batista, V. F. Andrioli, N. J. Schuch, (2017). Equatorial E region electric fields and sporadic E layer responses to the recovery phase of the November 2004 geomagnetic storm. *Journal of Geophysical Research: Space Physics*, 122, 12,517–12,533. https://doi.org/10.1002/2017JA024734.

Nogueira, P.A.B.; Abdu, M.A ; Batista, I. S.; Siqueira, P.M. (2011). Equatorial ionization anomaly and thermospheric meridional winds during two major storms over Brazilian

low latitudes. *Journal of Atmospheric and Solar-Terrestrial Physics*, v. 73, p. 1535-1543, doi: 10.1016/j.jastp.2011.02.008.

Otsuka, Y., T. Ogawa, A. Saito, T. Tsugawa, S. Fukao, and S. Miyazaki (2002), A new technique for mapping of total electron content using GPS network in Japan. *Earth Planets Space*, 54, 63-70, doi:10.1186/BF03352422

Pignalberi, A., M. Pezzopane, E. Zuccheretti (2014). Sporadic E layer at mid-latitudes: average properties and influence of atmospheric tides. *Annales Geophysicae*, 32, 1427-1440, doi: 0.5194/angeo-32-1427-2014.

Prasad, S. N. V. S., D. S. V. V. D. Prasad, K. K. Venkatesh, K. Niranjan, P. V. S. Rama Rao (2012). Diurnal and seasonal variations in sporadic E-layer (Es layer) occurrences over equatorial, low and mid latitude stations - A comparative study. *Indian Journal Radio Space Physics*, 41, 26-35.

Reddy, C. A. and M.M. Rao (1968). On the physical significance of the Es parameters *fb*Es, *ft*Es and *fo*Es. *Journal of Geophysical Research: Space Physics*, 21, 3, 331-341, doi: 10.1029/JA073i017p05627.

Reinisch, B.W., Galkin, I.A., Khmyrov, G.M., et al., 2009. The new Digisonde for research and monitoring applications. *Radio Science*, 44, doi: 10.1029/2008RS004115.

Resende, L. C. A., I. S. Batista, C. M. Denardini, A. J. Carrasco, V. F. Andrioli, J. Moro, P. P. Batista, S. S. Chen (2016), Competition between winds and electric fields in the formation of blanketing sporadic E layers at equatorial regions. *Earth Planets and Space*, 68:201, doi:10.1186/s40623-016-0577-z.

Resende, L. C. A., I. S. Batista, C. M. Denardini, P. P. Batista, A. J. Carrasco, V. F. Andrioli, J. Moro (2017a), Simulations of blanketing sporadic E-layer over the Brazilian sector driven by tidal winds. *Journal of Atmospheric and Solar-Terrestrial Physics*, 154, 104-114, doi:10.1016/j.jastp.2016.12.012.

Resende, L. C. A., I. S. Batista, C. M. Denardini, P. P. Batista, J. A. Carrasco, V. F. Andrioli, J. Moro (2017b). The influence of tidal winds in the formation of blanketing sporadic E-layer over equatorial Brazilian region. *Journal of Atmospheric and Solar-Terrestrial Physics*, 171, 64-67, doi:10.1016/j.jastp.2017.06.009.

Rishbeth, H., Ganguly, S., Walker, J. C. G. (1978). Field-aligned and field-perpendicular velocities in ionospheric F2-layer. *Journal of Atmospheric and Solar-Terrestrial Physics*, 40, 7, 767-784, doi: 10.1016/0021-9169(78)90028-4.

Santos, A., M., Abdu, M.A., Sobral, J. H., Koga, D., Nogueira, P. A. B., Candido, C. M. N. (2012). Strong longitudinal difference in ionospheric responsesover Fortaleza (Brazil) and Jicamarca (Peru) during the January 2005 magnetic storm, dominated by northward IMF. *Journal of Geophysical Research: Space Physics*, 117,A0833,1-10, doi: 10.1029/2012JA017604.

Santos, A., M., Abdu, M.A ; Souza, J. R., Sobral, J. H., Batista, I. S.; Denardini, C. M. (2016). Stormtime equatorial plasma bubble zonal drift reversal due to disturbance Hall electric

field over the Brazilian region: Disturbed zonal plasma drift. *Journal of Geophysical Research: Space Physics*, 121, 6,1-19, doi:10.1002/2015JA022179.

Sastri, J. H. (1988), Equatorial electric fields of ionospheric disturbance dynamo origin. *Annales Geophysicae*, 6, 635-642.

Takahashi, H., Wrasse, C. M, Denardini, C. M., Pádua, M. B., de Paula, E. R., Costa, S.M. A., Otsuka, Y., Shiokawa, K., Galera Monico, J. F., Ivo, A., N. Sant'Anna, N. (2016). Ionospheric TEC Weather Map Over South America. *Space Weather*, 14, 937–949, doi:10.1002/2016SW001474

Thorne, R. M. (2010). Radiation belt dynamics: The importance of wave-particle interactions, *Geophysical Research Letters*. 37, L22107, doi:10.1029/2010GL044990.

Whitehead, J. (1961). The formation of the sporadic-E in the temperate zones. *Journal of Atmospheric and Terrestrial Physics*, 20,1, 1155-1167, doi: 10.1016/0021-9169(61)90097-6.

Figure 1.

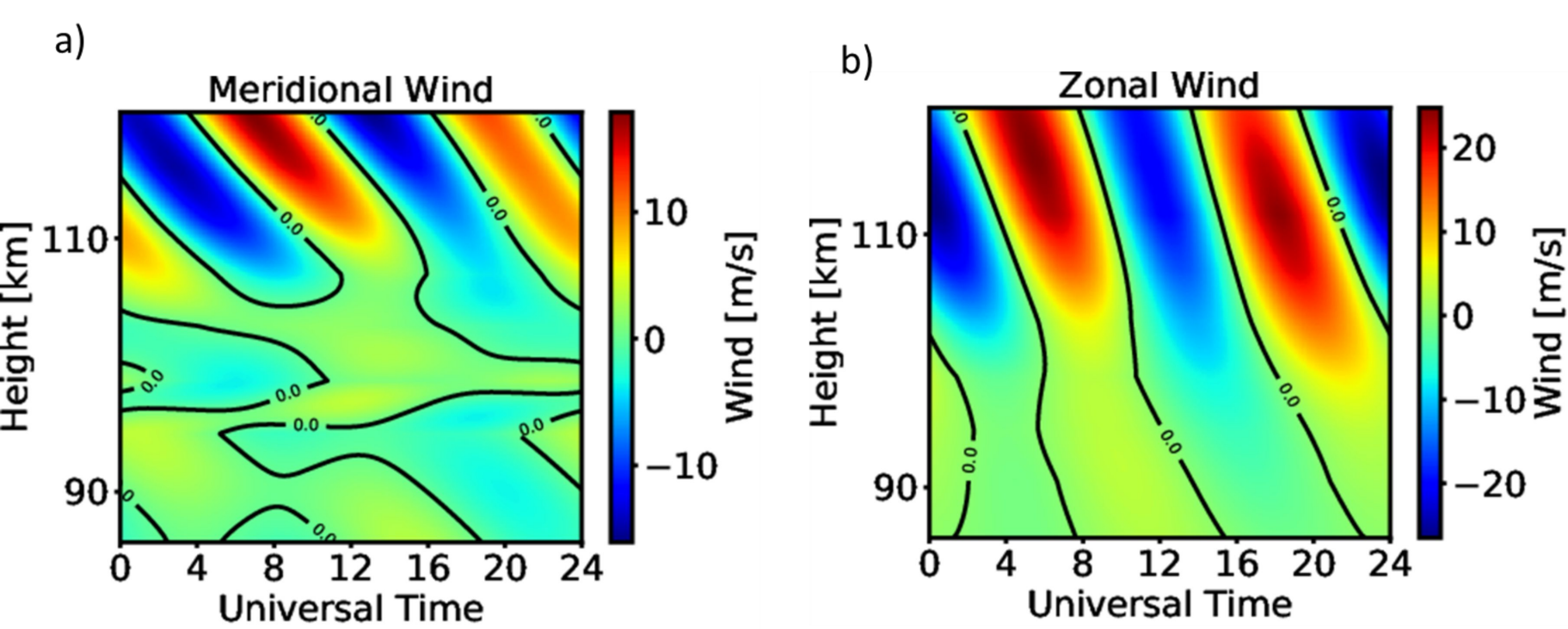
a)
Meridional Wind
Height [km]
110
90
0
4
8
12
16
20
24
Universal Time
10
0
−10
Wind [m/s]
b)
Zonal Wind
Height [km]
110
90
0
4
8
12
16
20
24
Universal Time
20
10
0
−10
−20
Wind [m/s]

Figure 2.

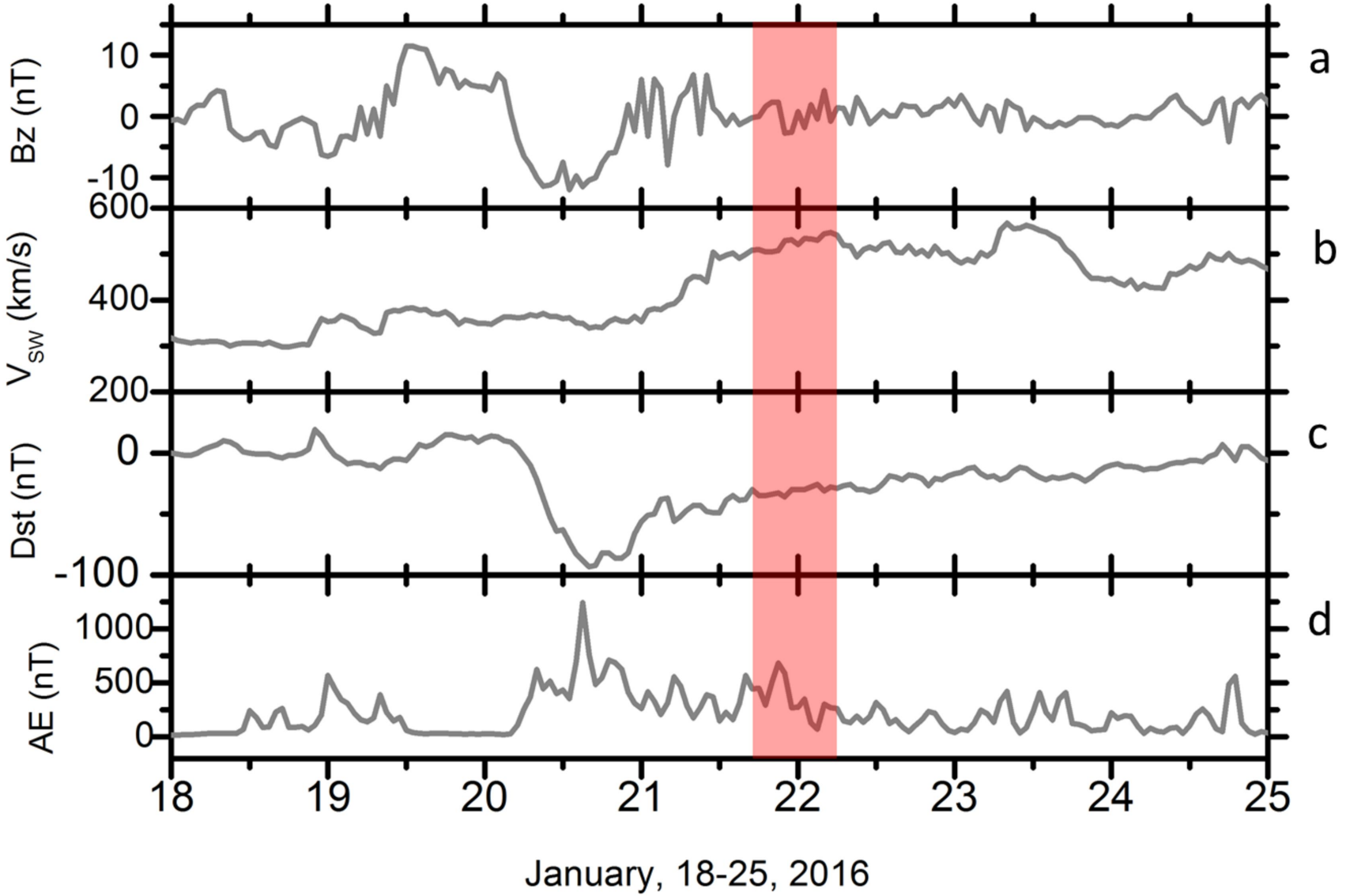
Bz (nT)
10
0
-10
a
V_{SW} (km/s)
600
400
200
b
Dst (nT)
0
-100
c
AE (nT)
1000
500
0
d
18
19
20
21
22
23
24
25
January, 18-25, 2016

Figure 3.

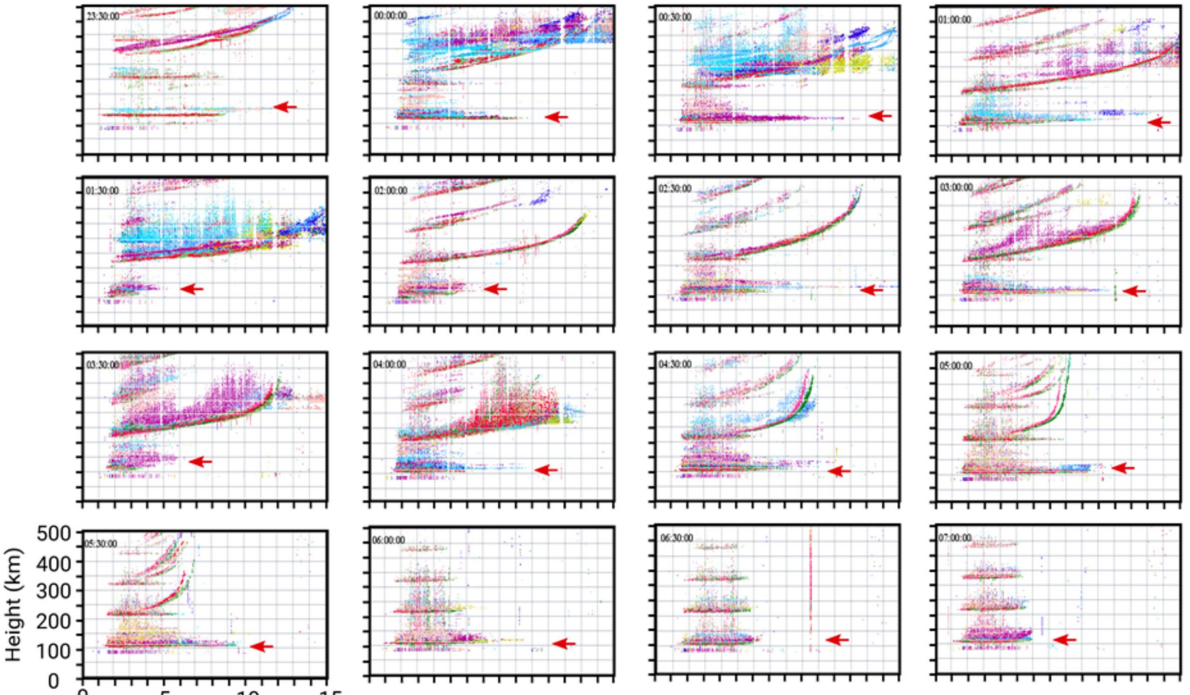
23:30:00
00:00:00
00:30:00
01:00:00
01:30:00
02:00:00
02:30:00
03:00:00
03:30:00
04:00:00
04:30:00
05:00:00
05:30:00
06:00:00
06:30:00
07:00:00
Height (km)
500
400
300
200
100
0
0
5
10
15
Frequency (MHz)

Figure 4.

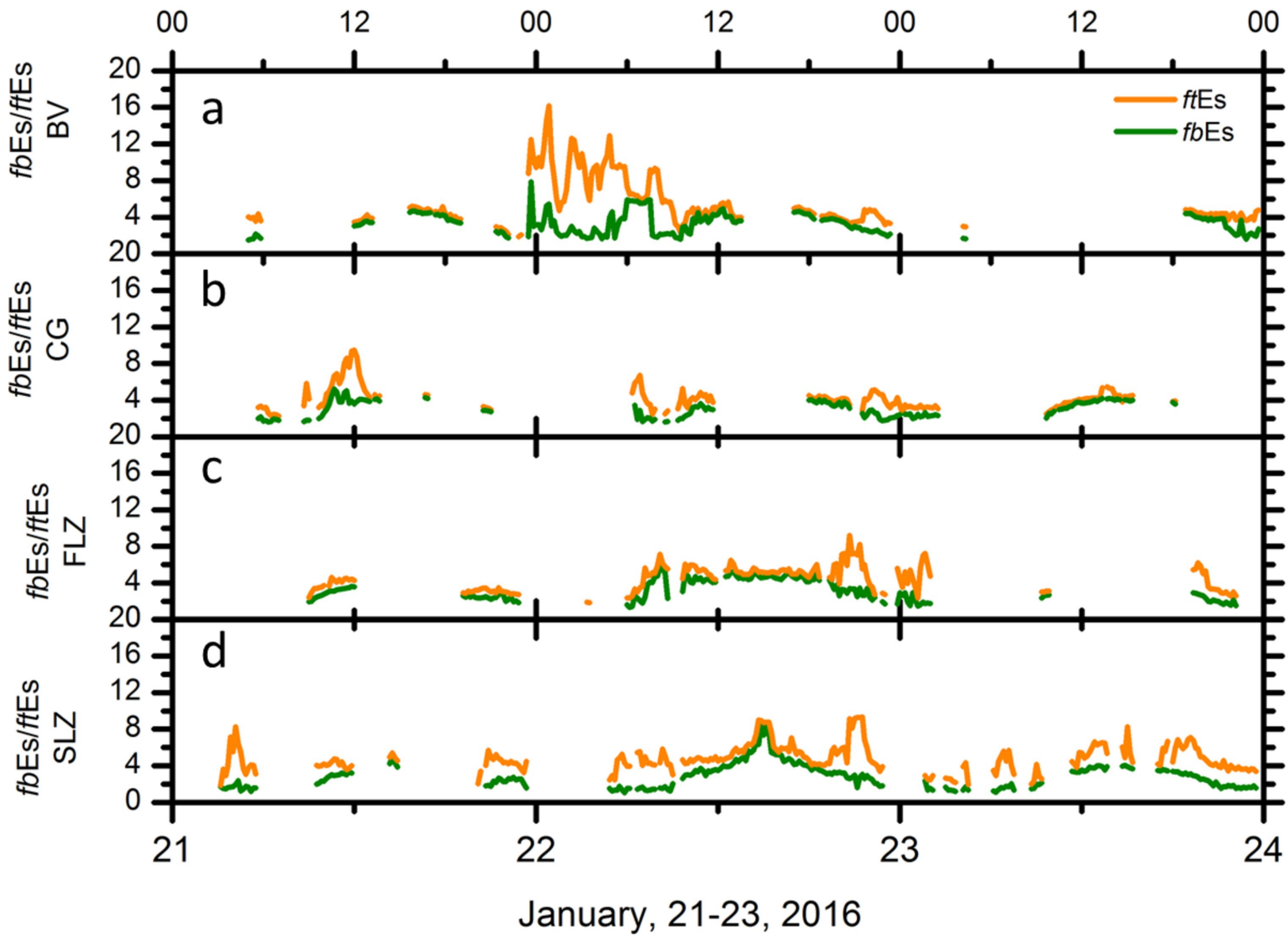
00
12
00
12
00
12
00
a
b
c
d
ftEs
fbEs
fbEs/ftEs
BV
fbEs/ftEs
CG
fbEs/ftEs
FLZ
fbEs/ftEs
SLZ
20
16
12
8
4
0
21
22
23
24
January, 21-23, 2016

Figure 5.

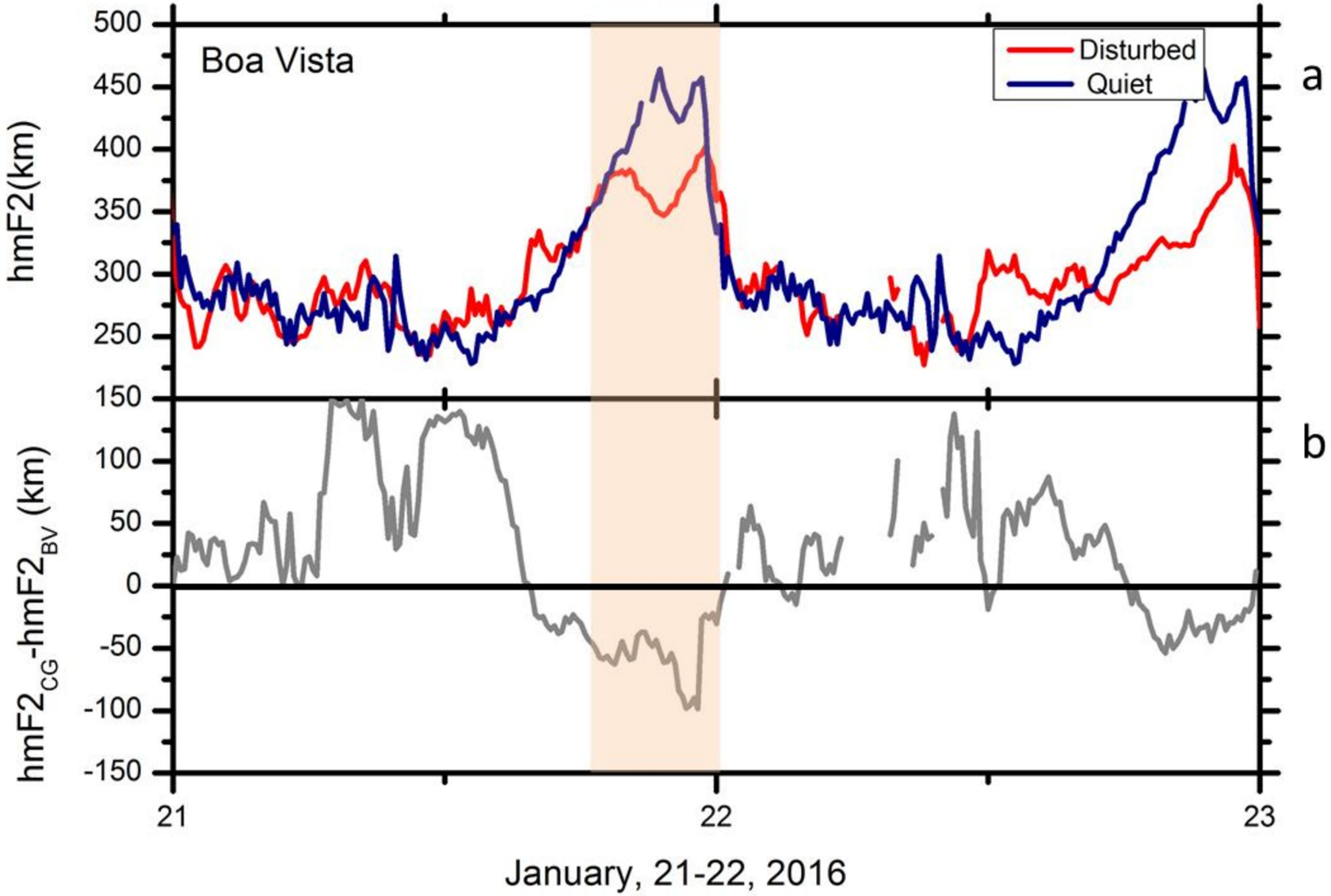
Boa Vista
Disturbed
Quiet
a
b
hmF2(km)
hmF2$_{CG}$-hmF2$_{BV}$ (km)
500
450
400
350
300
250
150
100
50
0
-50
-100
-150
21
22
23
January, 21-22, 2016

Figure 6.

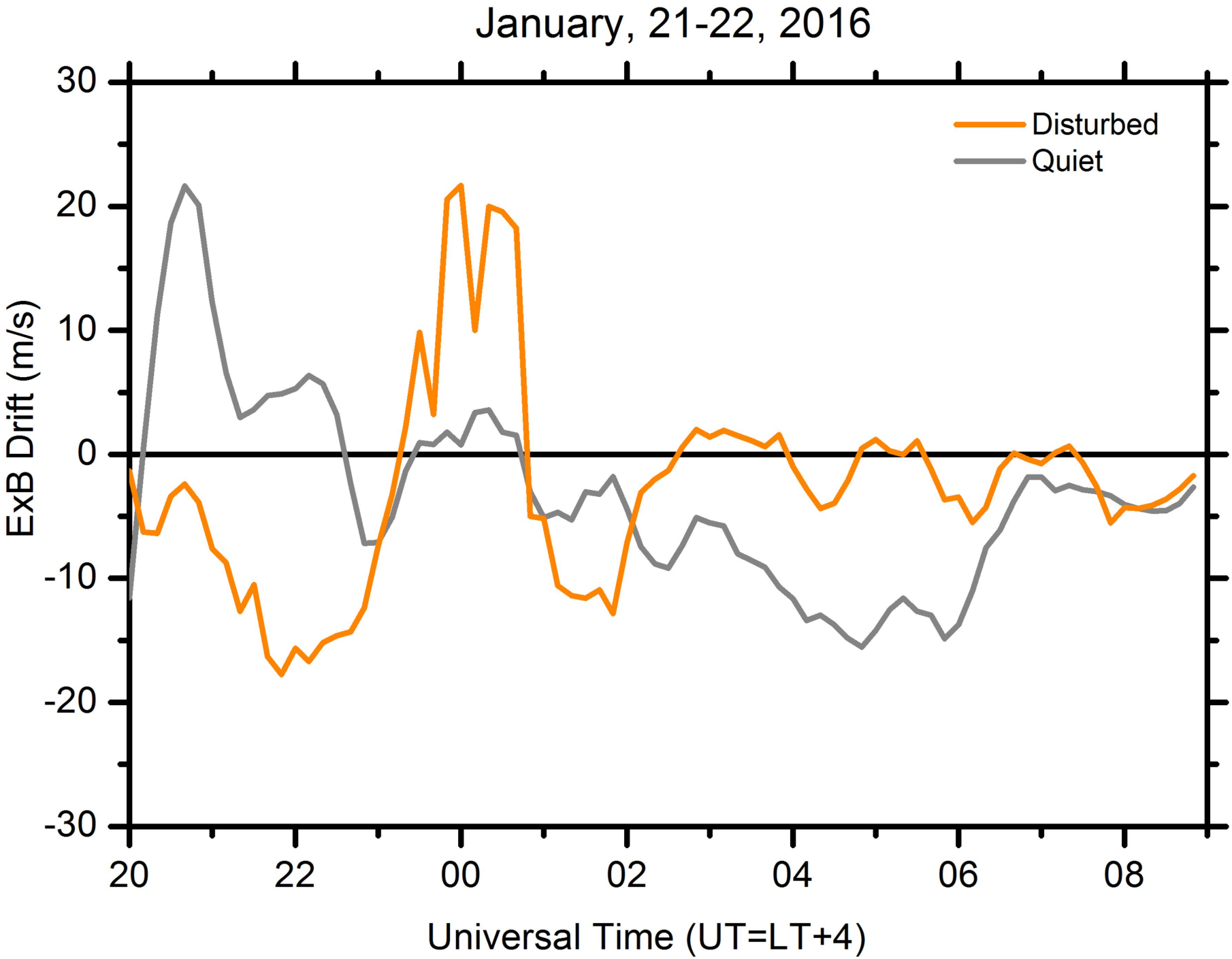
January, 21-22, 2016
Disturbed
Quiet
ExB Drift (m/s)
30
20
10
0
-10
-20
-30
20
22
00
02
04
06
08
Universal Time (UT=LT+4)

Figure 7.

January, 18, 2016

a)

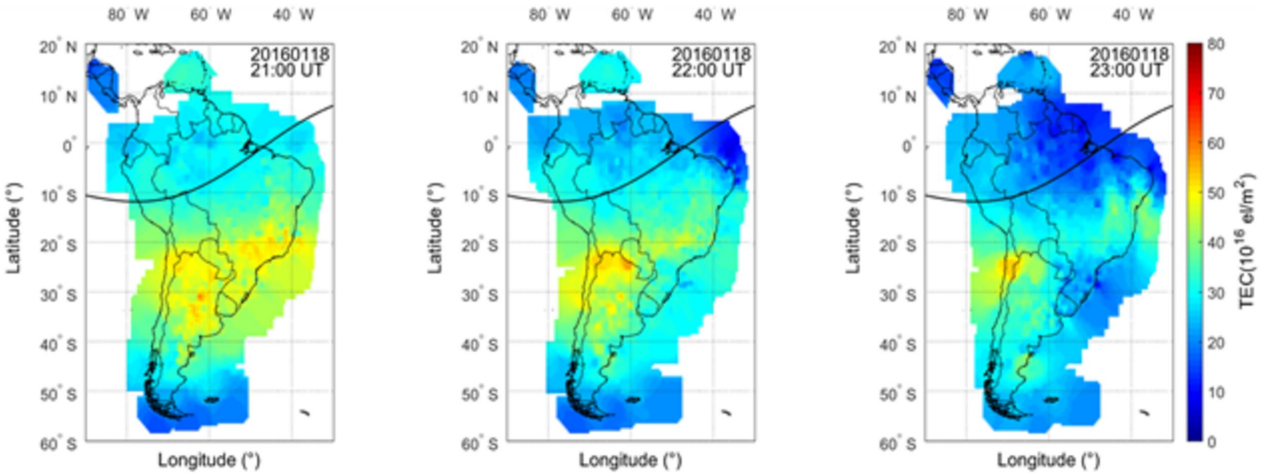

January, 21, 2016

b)

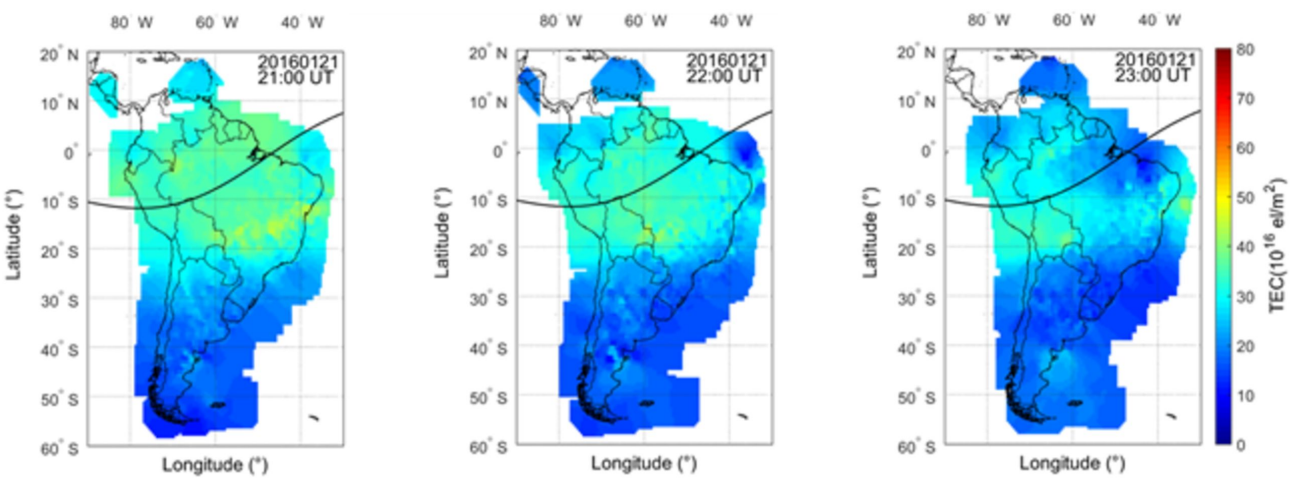

Figure 8.

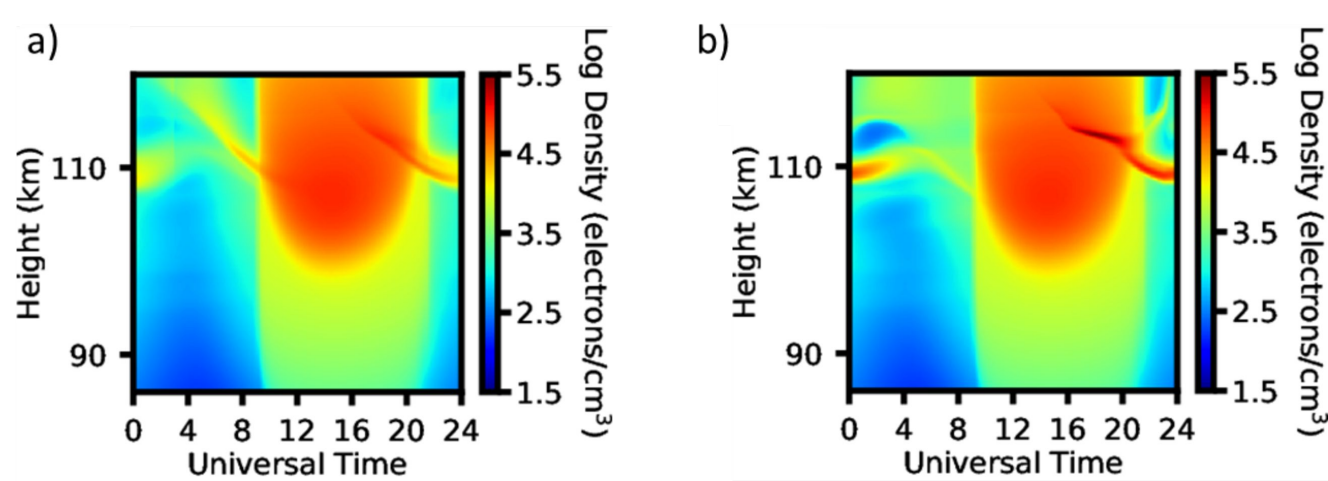
a)
b)
Height (km)
110
90
0 4 8 12 16 20 24
Universal Time
Log Density (electrons/cm^3)
5.5
4.5
3.5
2.5
1.5

Figure 9.

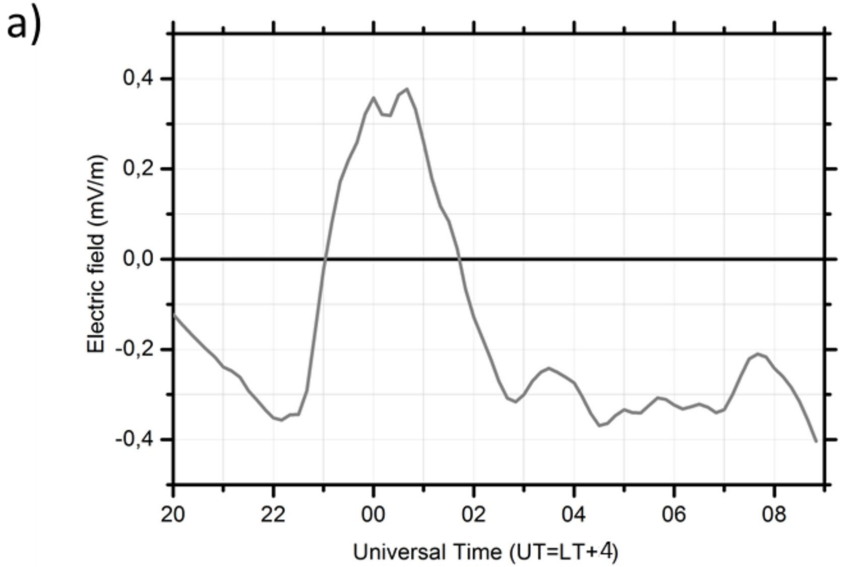
a)
0,4
0,2
0,0
-0,2
-0,4
Electric field (mV/m)
20
22
00
02
04
06
08
Universal Time (UT=LT+4)

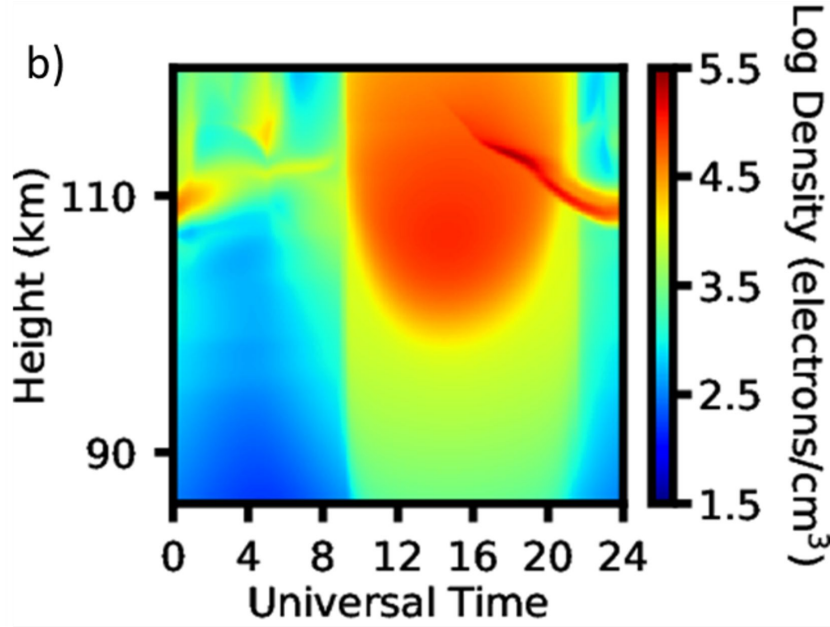
b)
Height (km)
110
90
0
4
8
12
16
20
24
Universal Time
5.5
4.5
3.5
2.5
1.5
Log Density (electrons/cm3)